Copy 481
RM L7I02a

CONFIDENTIAL

NASA TM X-3

CLASSIFICATION CHANGED
UNCLASSIFIED
To
By Authority of NASA TO 7455 Date 7-8-71

NASA TM X-3

TECHNICAL MEMORANDUM

X-3

Declassified by authority of NASA
Classification Change Notices No. 214
Dated ** 9-30-71

LONGITUDINAL STABILITY AND CONTROL CHARACTERISTICS OF A TWO-PLACE ALL-WEATHER FIGHTER AIRPLANE BETWEEN MACH NUMBERS OF 0.80 AND 2.00 OBTAINED FROM THE FLIGHT TEST OF A ROCKET-BOOSTED MODEL

By Earl C. Hastings, Jr., and Waldo L. Dickens

Langley Research Center
Langley Field, Va.

FACILITY FORM 602
N71-74024 (ACCESSION NUMBER)
50 (PAGES)
✓ (NASA CR OR TMX OR AD NUMBER)
(THRU)
None (CODE)
(CATEGORY)

NATIONAL AERONAUTICS AND SPACE ADMINISTRATION
WASHINGTON
August 1959

CONFIDENTIAL

UNCLASSIFIED
CONFIDENTIAL

NATIONAL AERONAUTICS AND SPACE ADMINISTRATION

TECHNICAL MEMORANDUM X-3

LONGITUDINAL STABILITY AND CONTROL CHARACTERISTICS OF A TWO-PLACE ALL-WEATHER FIGHTER AIRPLANE BETWEEN MACH NUMBERS OF 0.80 AND 2.00 OBTAINED FROM THE FLIGHT TEST OF A ROCKET-BOOSTED MODEL*

By Earl C. Hastings, Jr., and Waldo L. Dickens

SUMMARY

A rocket-boosted model of a two-place all-weather fighter airplane has been flight tested to determine longitudinal stability and control effectiveness between Mach numbers of 0.80 and 2.00.

The lift-curve slope increased at transonic speeds and had a maximum value at a Mach number of 0.98. At Mach numbers above 0.98, the lift-curve slope decreased gradually. There was a decrease in the lift coefficient at an angle of attack of 0° and a stabilator setting of 0° from a positive value at transonic speeds to a negative value at supersonic speeds.

There was no indication of pitch-up or decreasing static longitudinal stability over the lift-coefficient range covered although the pitching-moment curves were slightly nonlinear at negative lift coefficients. The aerodynamic-center location shifted rearward with increasing Mach number from a value of 36-percent mean aerodynamic chord at a Mach number of 0.80 to 60-percent mean aerodynamic chord between Mach numbers of 1.25 and 1.98.

Pitch damping was stabilizing at all Mach numbers between 0.9 and 2.0 although it decreased rapidly at transonic speeds. Throughout the Mach number range of the test, the all-movable stabilator remained an effective control for producing lift and pitching moment.

The external-drag coefficient had a maximum value of 0.042 between Mach numbers of about 1.30 and 1.60 and decreased slightly at Mach numbers between 1.60 and 1.90.

*Title, Unclassified.

CONFIDENTIAL

CONFIDENTIAL

INTRODUCTION

An investigation has been conducted by the Pilotless Aircraft Research Division of Langley Research Center to determine the aerodynamic characteristics of a two-place all-weather fighter airplane at transonic and supersonic speeds. This paper presents longitudinal-stability, control-effectiveness, and hinge-moment data between Mach numbers of 0.80 and 2.00 as obtained from the flight test of a rocket-boosted model with a pulsed stabilator. The flight test was conducted at the NASA Wallops Station.

L 2 1 0

SYMBOLS

The axis system shown in figure 1 indicates the positive directions of the forces, moments, and angles determined in the present investigation.

A	cross-sectional area, sq ft
$\frac{a_X}{g}, \frac{a_Y}{g}, \frac{a_Z}{g}$	accelerometer readings along X-, Y-, and Z-axis, respectively
b	wing span, ft
$\bar{c}$	mean aerodynamic chord, ft
C_D	drag coefficient based on theoretical wing area, $\frac{\text{Drag}}{qS}$
C_h	hinge-moment coefficient, $\frac{\text{Hinge moment}}{qS_t\bar{c}_t}$
C_L	lift coefficient based on theoretical wing area, $\frac{\text{Lift}}{qS}$
$C_{L,o}$	lift coefficient at wing angle of attack of 0° and stabilator setting of 0°
C_m	pitching-moment coefficient about center of gravity, $\frac{M_Y}{qS\bar{c}}$
$C_{m,o}$	pitching-moment coefficient at wing angle of attack of 0° and stabilator setting of 0°
$C_{m_q} = \frac{\partial C_m}{\partial \frac{\dot{\theta}\bar{c}}{2V}}$	per radian

CONFIDENTIAL

DECLASSIFIED

$C_{m_{\dot{\alpha}}} = \frac{\partial C_m}{\partial \frac{\dot{\theta}\bar{c}}{2V}}$, per radian

$C_{m_q} + C_{m_{\dot{\alpha}}}$ pitch damping derivative

C_n yawing-moment coefficient about center of gravity, $\frac{M_Z}{qSb}$

C_X force coefficient along X body axis, $\frac{a_X W}{gqS}$

C_Y force coefficient along Y body axis, $\frac{a_Y W}{gqS}$

C_Z force coefficient along Z body axis, $\frac{a_Z W}{gqS}$

g acceleration due to gravity, ft/sec^2

I_Y moment of inertia about Y-axis, slug-ft^2

I_Z moment of inertia about Z-axis, slug-ft^2

l length of fuselage, ft

m mass of model, slugs

M Mach number

M_X, M_Y, M_Z rolling, pitching, and yawing moments about X-, Y-, and Z-axes, respectively

P period of short-period oscillation, sec

q dynamic pressure, lb/sq ft

R Reynolds number based on wing mean aerodynamic chord

S theoretical wing area, sq ft

t time, sec

$T_{1/2}$ time to damp to one-half amplitude, sec

V velocity, ft/sec

CONFIDENTIAL

W	weight, lb
x	fuselage station measured from nose, ft
X,Y,Z	rectangular coordinate axes
α	angle of attack of X-axis, deg or radians
β	angle of sideslip, deg
γ	flight-path angle, deg
δ	incidence angle of stabilator with respect to wing, deg
ϵ	downwash angle at stabilator, deg
ζ	critical-damping ratio
θ	angle between horizontal and X-axis, radians
μ	relative-density factor, $\frac{m}{\rho S b}$
ρ	mass density of air, slugs/cu ft
ϕ	roll angle, deg
ψ	yaw angle, deg

Subscripts:

b	base
ext	external
i	internal
t	stabilator
tot	total
w	wing
θ	pitch
ψ	yaw

L 2 1 0

CONFIDENTIAL

Derivatives are expressed in this manner: $C_{L_\alpha} = \frac{\partial C_L}{\partial \alpha}$, $C_{h_\delta} = \frac{\partial C_h}{\partial \delta}$, and so forth. A dot over a symbol indicates the first derivative with respect to time, and two dots indicate the second derivative with respect to time.

MODEL AND INSTRUMENTATION

Model

A three-view drawing of the model is shown in figure 2, and a photograph is shown in figure 3. Table I presents the geometric and mass characteristics of the model, and figure 4 shows the normal cross-sectional-area distribution.

A hydraulically actuated duralumin stabilator was used to pulse the model in pitch by operating with approximately a square wave motion between settings of 0° and -9° with respect to the wing. The stabilator timing sequence was controlled by an electrically operated solenoid valve which regulated the flow of hydraulic fluid to the stabilator piston. Due to the decrease in model frequency at the lower test Mach numbers, the dwell times in the 0° and -9° positions were increased by using a pressure-operated switch to change the stabilator pulsing rate in flight at the desired time.

Inlet, duct, and base geometric characteristics of the model discussed herein were the same as those of a similar rocket-boosted model flown in a previous test to determine the drag at low lift coefficients of this configuration. For this reason the ducts and bases were not instrumented in this test since duct mass-flow ratio, internal drag, total-pressure recovery, and base drag should be the same as that obtained from the previous test.

An M5 JATO Nike rocket motor was used to boost the model to the desired Mach number. At burnout, the model separated from the booster and coasted through the test Mach number range with the stabilator continuously pulsing. All the data presented in this paper were obtained during this coasting phase of the flight. A photograph of the model-booster combination prior to firing is shown in figure 5.

Instrumentation

A nine-channel telemeter system was used in this investigation. The quantities determined from the model telemeter during flight were: accelerations along the X, Y, and Z body axes measured near the center

of gravity, angles of attack and sideslip, stabilator setting, stabilator hinge moment, normal acceleration at a station aft of the center of gravity, and free-stream total pressure. These quantities were transmitted from the model to a ground receiving station during flight.

Required atmospheric conditions and winds aloft were determined by the use of a rawinsonde balloon released near the time of firing. The position of the model in space was established with an NACA modified SCR 584 tracking radar unit. During the flight test, the rolling velocity of the model was measured by utilizing the polarized telemeter signal and a special rotating receiving antenna.

L 2 1 0

REDUCTION OF DATA

Reference 1 presents a discussion of the assumptions made and the method used in the reduction of longitudinal-stability data from a free-flight model abruptly disturbed in pitch. This method of analysis assumed a two-degree-of-freedom motion involving translation normal to the flight path and rotation in pitch about the center of gravity and was used in reducing most of the static- and dynamic-longitudinal-stability and control-effectiveness data presented herein. By using the method of reference 1, it was also possible to determine the pitching-moment coefficient C_m directly by using two normal accelerometers (one at the center of gravity and one rearward of the center of gravity), to find pitching acceleration $\ddot{\theta}$, and to compute C_m by the following relationship

$$C_m = \frac{I_Y \ddot{\theta}}{qS\bar{c}} - \left(C_{m_q} + C_{m_{\dot{\alpha}}}\right) \frac{\dot{\alpha}\bar{c}}{2V} - C_{m_q} \frac{\dot{\gamma}\bar{c}}{2V}$$

where the last two terms in the equation are pitching moments due to pitch damping of the free-flight model.

The telemeter records of the test showed small sinusoidal lateral oscillations shortly after separation and at the lower Mach numbers. By assuming a single degree of freedom in sideslip, it was possible to determine a directional-stability parameter C_{n_β} by using the period of this oscillation in the equation

$$C_{n_\beta} = \frac{4\pi^2 I_Z}{57.3 qSbP_\psi^2}$$

CONFIDENTIAL

As in reference 1, the total lift and drag coefficients were computed as

$$C_L = -C_Z \cos \alpha + C_X \sin \alpha$$

$$C_{D,tot} = -C_Z \sin \alpha - C_X \cos \alpha$$

CORRECTIONS AND ACCURACY

Corrections

Prior to the flight test of the model, a static-load test was applied to the stabilator to determine the twist per unit load for loads applied at various spanwise and chordwise stations as discussed in reference 1. With these data, the indicated stabilator deflection, which was measured in flight at the root chord, was adjusted to the deflection at the stabilator mean aerodynamic chord. Therefore, the values of stabilator deflection presented in this paper are the angles between the wing and the stabilator mean aerodynamic chord.

Angles of attack and sideslip were measured with respect to the X-axis with a vane located ahead of the model, and the values indicated were, therefore, influenced by pitching and yawing velocity. These indicated values were corrected for these effects by the method discussed in reference 1, and are presented herein as steady-state values of angles of sideslip and angles of attack.

In addition to the pitching correction made to the value of angle of attack indicated by the vane, corrections for the dynamic effect of stabilator angle of attack also had to be made when hinge-moment data were reduced. The static angle of attack at the stabilator used in determining hinge-moment characteristics was calculated from the relation

$$\alpha_{static} = \alpha + \frac{l_t}{V}\left[\left(1 - \frac{d\epsilon}{d\alpha}\right)\dot{\alpha} + \dot{\gamma}\right]$$

where l_t was the distance in feet between the model center of gravity and the estimated stabilator center of pressure. A constant 1.0° increment was also added to the corrected angle-of-attack readings so that angle of attack is given relative to the wing (which had a 1.0° incidence angle) rather than to the X-body axis.

CONFIDENTIAL

Since it was not possible to locate all of the accelerometers directly at the model center of gravity, the readings of these instruments were also affected by the pitching and yawing motions of the model. Prior to firing, the location of the accelerometers was determined, and the indicated readings were corrected for these motions by the method discussed in reference 1.

Inertia corrections to hinge-moment data due to static unbalance were not made because the magnitude of this unbalance was not known.

L 2 1 0

Accuracy

The following table presents what are believed to be reasonable values of absolute accuracy for some of the basic test parameters at Mach numbers of 0.80 and 2.00:

	M = 0.80	M = 2.00
M	±0.020	±0.010
C_h	±0.0004	±0.00003
C_X	±0.002	±0.001
C_Y	±0.03	±0.01
C_Z	±0.03	±0.01
α, deg	0.5 ± 0.30	0.5 ± 0.30
β, deg	0.5 ± 0.30	0.5 ± 0.30
δ, deg	±0.10	±0.10
C_m	----------	±0.005

(At a Mach number of 0.80, no value for C_m is given because values of C_m for Mach numbers of less than 1.01 were felt to be unreliable, and no data involving the magnitude of C_m have been presented in that speed range.) The accuracy values are based largely on past experience with similar tests and were determined by comparison of several sources of data. In some cases, when no comparative data were available, the total accuracy has been estimated on the basis of instrument error.

RESULTS AND DISCUSSION

Test Conditions

Figure 6 shows the variation of the parameters q, V, μ, R, and ρ with Mach number between 0.80 and 2.00. The relative density

factor μ is based on wing area and wing span, and the Reynolds number R is based on the length of the wing mean aerodynamic chord.

Lift

Some typical variations of C_L with α_w are presented in figure 7 and were obtained at various Mach numbers and stabilator settings. The lift curves shown in figure 7 are linear except at $M = 0.85$ where C_L is nonlinear with α_w above $C_L = 0.65$ and at $M = 1.98$ where nonlinearity is shown at negative lift coefficients greater than $C_L = -0.06$.

Figure 8 presents the variation of C_{L_α} with Mach number between 0.81 and 1.98. These values of C_{L_α} were obtained at low lift coefficients. Although the configuration of the present test had a stabilator dihedral angle of -23.25°, a comparison is made in figure 8 with unpublished data from Langley Unitary Plan wind tunnel (UPWT) test of a similar configuration with a stabilator dihedral angle of -15°, and excellent agreement is shown at $M = 1.57$ and 1.87. The lift-curve slope has a maximum value of 0.076 at $M \approx 0.98$ and decreases gradually with increasing Mach number. Values of lift coefficient for a wing angle of attack of 0° and stabilator setting of 0° $C_{L,o}$ are plotted against Mach number in figure 9. The value of $C_{L,o}$ decreases with increasing Mach number from a value of 0.091 at $M = 0.81$ to a value of -0.015 at $M = 1.98$.

Pitching Moment

Figure 10 presents typical plots of C_m as a function of C_L for various Mach numbers and stabilator settings. All of the values of C_m are about the center of gravity which was located $0.199\bar{c}_w$. Throughout the test Mach number range, the pitching-moment curves are slightly nonlinear for negative values of C_L, but none of the curves showed any pitch-up or decrease in longitudinal stability with increasing lift coefficients over the lift-coefficient range covered by the test.

The pitching-moment coefficient at stabilator setting of 0° and wing angle of attack of 0° $C_{m,o}$ is plotted as a function of Mach number in figure 11. As Mach number increases from about 1.30 to 1.98, $C_{m,o}$ varies from about -0.009 to 0.008. Unpublished data from the Langley Unitary Plan wind tunnel are also shown in this figure for comparison at Mach numbers of 1.57 and 1.87.

Figure 12 presents the period in pitch P_θ of the model as determined from the model pitching oscillations. These values were used in a two-degree-of-freedom analysis to determine the aerodynamic-center location by the method discussed in reference 1. Figure 13 shows the variation of aerodynamic-center location with Mach number obtained by this method and also by using the slopes of pitching-moment curves similar to those of figure 10 at low lift. Agreement between the values is good throughout the Mach number range. The aerodynamic-center location moves rearward in the transonic speed range from a value of 36-percent $\bar{c}_w$ at $M = 0.80$ to a value of 60-percent $\bar{c}_w$ at $M = 1.25$. Between $M = 1.25$ and 1.98 the aerodynamic-center location is constant at 60-percent $\bar{c}_w$.

L 2 1 0

Also plotted in figure 13 are estimates of aerodynamic-center location for a configuration with the same stabilator dihedral angle as that of the model. The estimates and the rocket-model data agree very well between $M = 0.8$ and $M = 1.0$ and between about $M = 1.5$ and $M = 2.0$. In the Mach number range from 1.0 to 1.5, however, the estimates show a more forward aerodynamic-center location and a more gradual rearward movement with Mach number than the rocket model experienced. Values of aerodynamic-center location as determined from the test in the Langley Unitary Plan wind tunnel (stabilator dihedral angle of -15°) are also plotted on figure 13 at $M = 1.57$ and $M = 1.87$ and show good agreement with the present test at both of these Mach numbers.

Longitudinal Trim

Longitudinal trim characteristics of the model are presented in figures 14 and 15 which show, respectively, variations of trim wing angle of attack and trim lift coefficient with Mach number. These data are for the model with a center-of-gravity location at $0.199\bar{c}_w$ and stabilator settings of approximately 0° and -8° and were obtained from lift and pitching-moment curves and from the time history of the model motions.

Dynamic Longitudinal Stability

The damping-in-pitch characteristics of the model are given by the parameters $T_{1/2}$ and $C_{m_q} + C_{m_{\dot{\alpha}}}$ and are presented as functions of Mach number in figures 16 and 17, respectively. Figure 17 indicates that pitch damping is stabilizing throughout the test Mach number range. A decrease in pitch damping is shown at transonic speeds followed by an increase between Mach numbers of 1.15 and 1.30. Above $M = 1.35$ there is a steady decrease with increasing Mach number to $M = 1.89$.

The critical-damping ratio ζ, computed from the pitch period of figure 12 and from $T_{1/2}$ of figure 16, is plotted as a function of Mach number in figure 18. If a full-scale airplane had the same relative density factor as the model (fig. 6), the values of ζ shown in figure 18 would be applicable to the full-scale airplane with no artificial pitch damping between altitudes of 50,000 and 62,000 feet.

Longitudinal Control Effectiveness

The effectiveness of the all-movable stabilator hinged at $0.41\bar{c}_t$ in producing lift and pitching moment is shown in figures 19 and 20. The values of C_{L_δ} shown in figure 19 were obtained from the increment in C_L due to control movement at a constant wing angle of attack. Values of C_{L_δ} increase from 0.005 at $M = 0.88$ to a maximum of about 0.012 at $M = 1.03$. As Mach number increases, C_{L_δ} decreases to a value of 0.004 at $M = 1.92$.

Figure 20 shows the variation with Mach number of values of stabilator pitching effectiveness C_{m_δ} from the rocket model test and from estimates for the configuration with the same stabilator dihedral angle as that of the model. Good agreement is shown between the two sources of data in the Mach number range from 1.02 to 1.92.

Figures 21 and 22 present two additional longitudinal-control-effectiveness parameters obtained from this test. The change in trim angle of attack per degree of stabilator deflection $\left(\frac{\Delta\alpha}{\Delta\delta}\right)_{trim}$ of figure 21 shows a steady decrease between $M = 0.94$ and 1.95. This same trend is also shown for the change in trim lift coefficient per degree of stabilator deflection presented in figure 22. Although all of the longitudinal-control data presented show a decrease in effectiveness with increasing supersonic Mach number, the stabilator remains an effective control for producing lift and pitching moment throughout the Mach number range covered by this test.

Stabilator Hinge Moment

Some typical plots of stabilator hinge-moment coefficient with wing angle of attack are shown in figure 23 and indicate typical fairing of data points over small values of α_w to obtain the slope C_{h_α} presented in figure 24. The values of C_h are plotted over a complete cycle

against values of α_w which have been corrected for model dynamic effects. Figure 24 indicates that values of C_{h_α} obtained from this method agree very well with unpublished data over the Mach number range of the test although the accuracy of the present data is not known because of the unknown inertia correction to the measured hinge moment.

By taking the increment in C_h due to the increment in stabilator deflection at a constant α_w, values of C_{h_δ} were determined and are plotted against Mach number in figure 25. The comparison with unpublished data shown in this figure indicates that, between $M = 0.87$ and $M \approx 1.40$, the rocket-model values of C_{h_δ} are more negative than the unpublished data, but, between $M = 1.40$ and 1.95, agreement between the two sources of data is good.

L 2 1 0

Drag

Figure 26 presents plots of $C_{D,tot}$ as a function of C_L for stabilator settings of about 0° and -8°, where the values of $C_{D,tot}$ contain both internal and base drag. Values of internal- and base-drag coefficients presented in figure 27 were obtained from a previous test of a rocket-boosted model with the same internal and base geometry. The dashed lines in this figure are estimates of $C_{D,i}$ and $C_{D,b}$ for Mach numbers at which they were not obtained in the previous test. Figure 28 presents minimum values of $C_{D,tot}$ plotted against Mach number; the values shown were taken from the drag plots of figure 26.

Figure 29 shows $C_{D,ext}$ obtained by subtracting $C_{D,i}$ and $C_{D,b}$ from the faired values of $C_{D,tot}$. The minimum external-drag coefficient has a value of 0.010 below $M = 0.85$ and increases to a maximum value of 0.042 between $M = 1.30$ and $M = 1.60$. This is followed by a slight decrease in $C_{D,ext}$ with increasing Mach number to a value of 0.040 at $M = 1.90$. Data from the Unitary Plan wind-tunnel test are also plotted on figure 29 at $M = 1.57$ and $M = 1.87$ and excellent agreement is shown at both of these Mach numbers. The effect of difference in test Reynolds number has not been investigated in making this comparison.

Static Directional Stability

Throughout a portion of the flight test, the model experienced small lateral oscillations which made it possible to make a quantitative

analysis of the static directional stability. Figure 30 presents values of the side force derivative C_{Y_β} which were obtained between $\beta = \pm 1.5^\circ$ and for angles of attack of less than 4°. Values of C_{Y_β} from the Unitary Plan wind tunnel are also shown at $M = 1.57$ and 1.87 for a model with a -15° stabilator dihedral angle.

In order to determine the static-directional-stability parameter C_{n_β}, the periods of the yawing oscillations were obtained and used with the moment of inertia in yaw to calculate an approximate C_{n_β} by the single-degree-of-freedom method described in an earlier section of this paper. The values of yaw period P_ψ for both low and moderate angle-of-attack ranges are shown in figure 31. Figure 32 presents values of C_{n_β} calculated from the measured periods of figure 31 and also data from the Unitary Plan wind tunnel at $M = 1.57$ and $M = 1.87$ for the model with stabilator dihedral of -15°. For comparative purposes these data have been referred to the same moment center as the rocket model. The data of figure 32 show that the model was statically stable throughout the test Mach number range.

L 2 1 0

CONCLUSIONS

Results from the flight test of a rocket-boosted model of a two-place all-weather fighter airplane indicate the following conclusions:

1. The lift-curve slope increased in the transonic speed range to a maximum value of 0.076 at a Mach number of 0.98 and then decreased gradually with increasing Mach number. The lift coefficient at a wing angle of attack of 0° and stabilator setting of 0° decreases from 0.091 at a Mach number of 0.81 to -0.015 at a Mach number of 1.98.

2. Throughout the range of Mach numbers covered by this test, there was no indication of pitch-up or decreasing static longitudinal stability over the lift range covered although the pitching-moment curves are slightly nonlinear at negative lift coefficients.

3. The aerodynamic-center location moved rearward in the transonic speed range from a point at 36 percent of the mean aerodynamic chord at a Mach number of 0.80 to a position at 60 percent of the mean aerodynamic chord at a Mach number of 1.25. At Mach numbers between 1.25 and 1.98, the location of the aerodynamic center was constant at 60 percent of the mean aerodynamic chord.

4. Pitch damping was stabilizing throughout the test Mach number range although it decreased rapidly at transonic speeds. The maximum value of pitch damping in the supersonic Mach number range occurred at a Mach number of about 1.35.

5. The all-moveable stabilator was an effective control for producing lift and pitching moment throughout the Mach number range of the test although effectiveness decreased with increasing supersonic Mach numbers.

6. Values of the minimum external-drag coefficient increased with increasing Mach number to a maximum of 0.042 at a Mach number of about 1.30. There was a slight decrease in external drag coefficient at Mach numbers between 1.60 and 1.90. At a Mach number of 1.90, the external drag coefficient had a value of 0.040.

L
2
1
0

Langley Research Center,
National Aeronautics and Space Administration,
Langley Field, Va., February 10, 1959.

REFERENCES

1. Gillis, Clarence L., and Mitchell, Jesse L.: Determination of Longitudinal Stability and Control Characteristics From Free-Flight Model Tests With Results at Transonic Speeds for Three Airplane Configurations. NACA Rep. 1337, 1957.

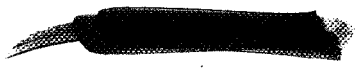

TABLE I.- GEOMETRIC AND MASS CHARACTERISTICS OF A MODEL OF A TWO-PLACE ALL-WEATHER FIGHTER

Wing:	
Area (theoretical), sq ft	8.96
Area (including leading-edge extension), sq ft	9.10
Span, ft	4.99
Root chord (center line of model), ft	3.05
Tip chord (theoretical), ft	0.51
Mean aerodynamic chord, ft	2.08
Incidence angle, deg	+1.00
Sweepback of leading edge, deg	51.40
Sweepback of quarter-chord line, deg	45.00
Sweepback of trailing edge, deg	13.50
Taper ratio	0.167
Aspect ratio	2.82
Dihedral (inboard of spanwise station 20.8), deg	0
Dihedral (outboard of spanwise station 20.8), deg	12.00
Airfoil section at root	NACA 0006.4-64 (Modified)
Airfoil section at tip	NACA 0003.0-64 (Modified)
Stabilator (dimensions in chord plane):	
Total area, sq ft	1.63
Span, ft	2.30
Aspect ratio	3.30
Taper ratio	0.20
Sweepback of leading edge, deg	42.25
Sweepback of quarter-chord line, deg	35.50
Hinge-line location, percent $\bar{c}$	41.0
Dihedral, deg	-23.25
Root chord (center line of model), ft	1.16
Tip chord (theoretical), ft	0.23
Mean aerodynamic chord, ft	0.80
Distance between model center of gravity and stabilator hinge line, ft	3.40
Airfoil section at root	NACA 0003.7-64 (Modified)
Airfoil section at tip	NACA 0003.0-64 (Modified)
Vertical tail:	
Area (as indicated in fig. 1), sq ft	1.15
Taper ratio	0.23
Aspect ratio	0.60
Height (above fuselage and trailing-edge intersection), ft	0.83
Root chord, ft	2.24
Tip chord, ft	0.51
Mean aerodynamic chord, ft	1.56
Duct:	
Inlet capture area, sq in./side	11.62
Exit area, sq in./side	7.50
Base area, sq in./side	11.80
Fuselage and nacelle:	
Length, ft	7.28
Width (maximum), ft	1.16
Depth (maximum), ft	0.82
Maximum frontal area (fuselage alone), sq ft	0.43
Maximum frontal area (including nacelles), sq ft	0.78
Weight and balance:	
Weight, lb	447.0
Wing loading, lb/sq ft	49.88
Center of gravity (percent $\bar{c}$)	19.93
Moment of inertia in pitch, slug-ft^2	39.75
Moment of inertia in yaw, slug-ft^2	43.04
Moment of inertia in roll, slug-ft^2	5.33

CONFIDENTIAL

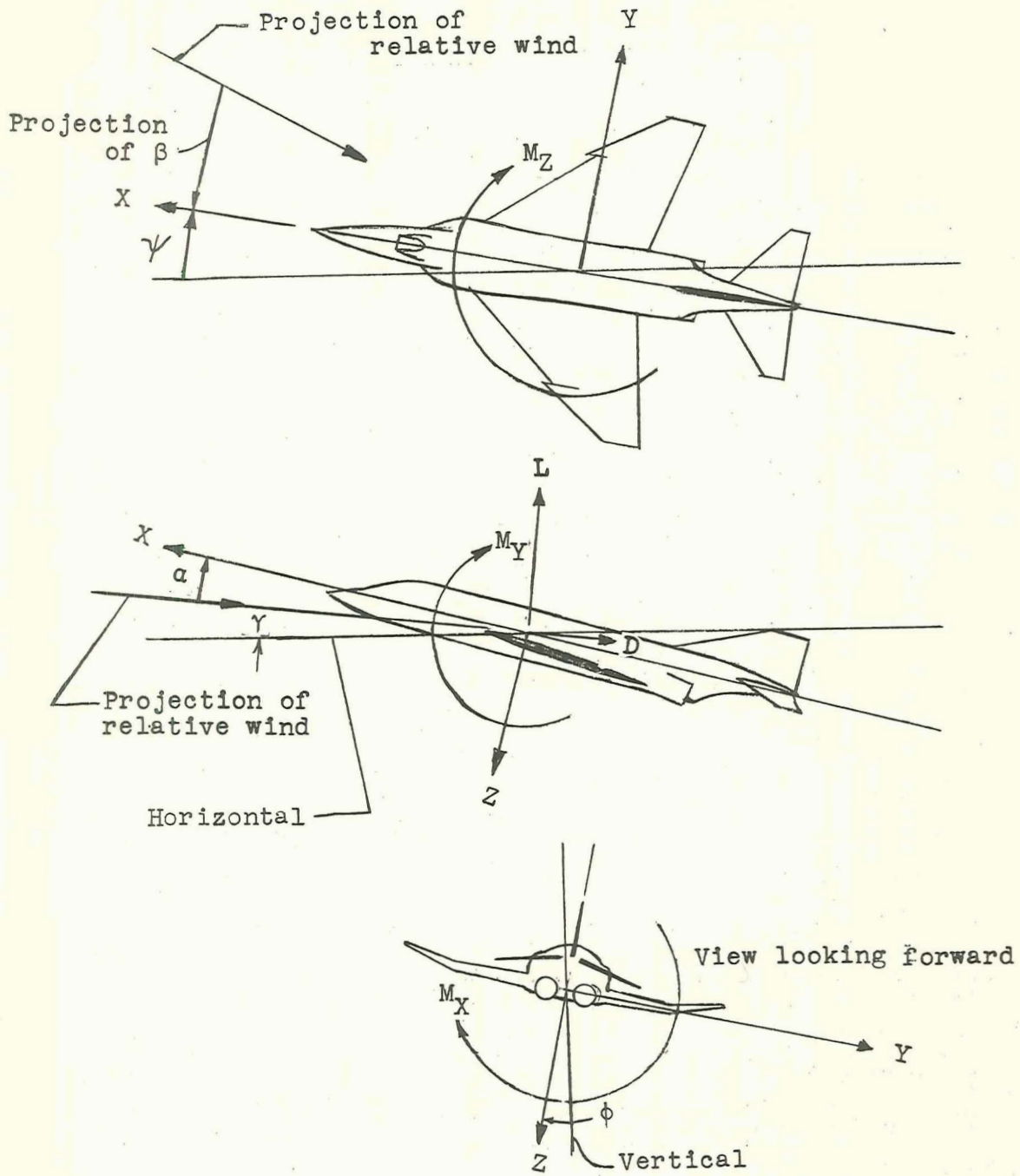

Figure 1.- Sketch showing axis system. Each view presents a plane of the axis system as viewed along the third axis. Arrows indicate positive directions of forces, moments, and angles.

CONFIDENTIAL

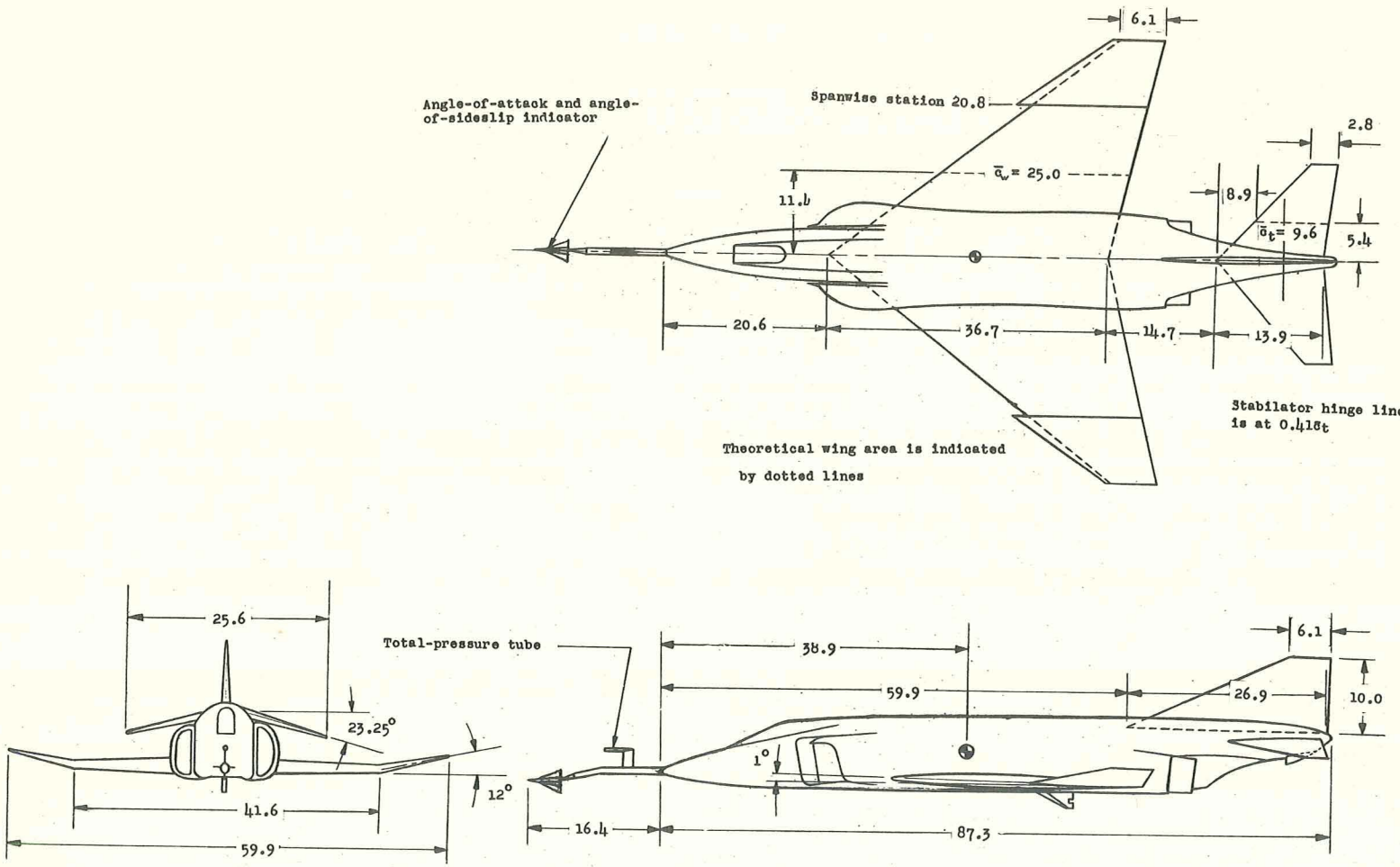

Figure 2.- Three-view drawing of model. All dimensions are in inches.

CONFIDENTIAL
CONFIDENTIAL

CONFIDENTIAL

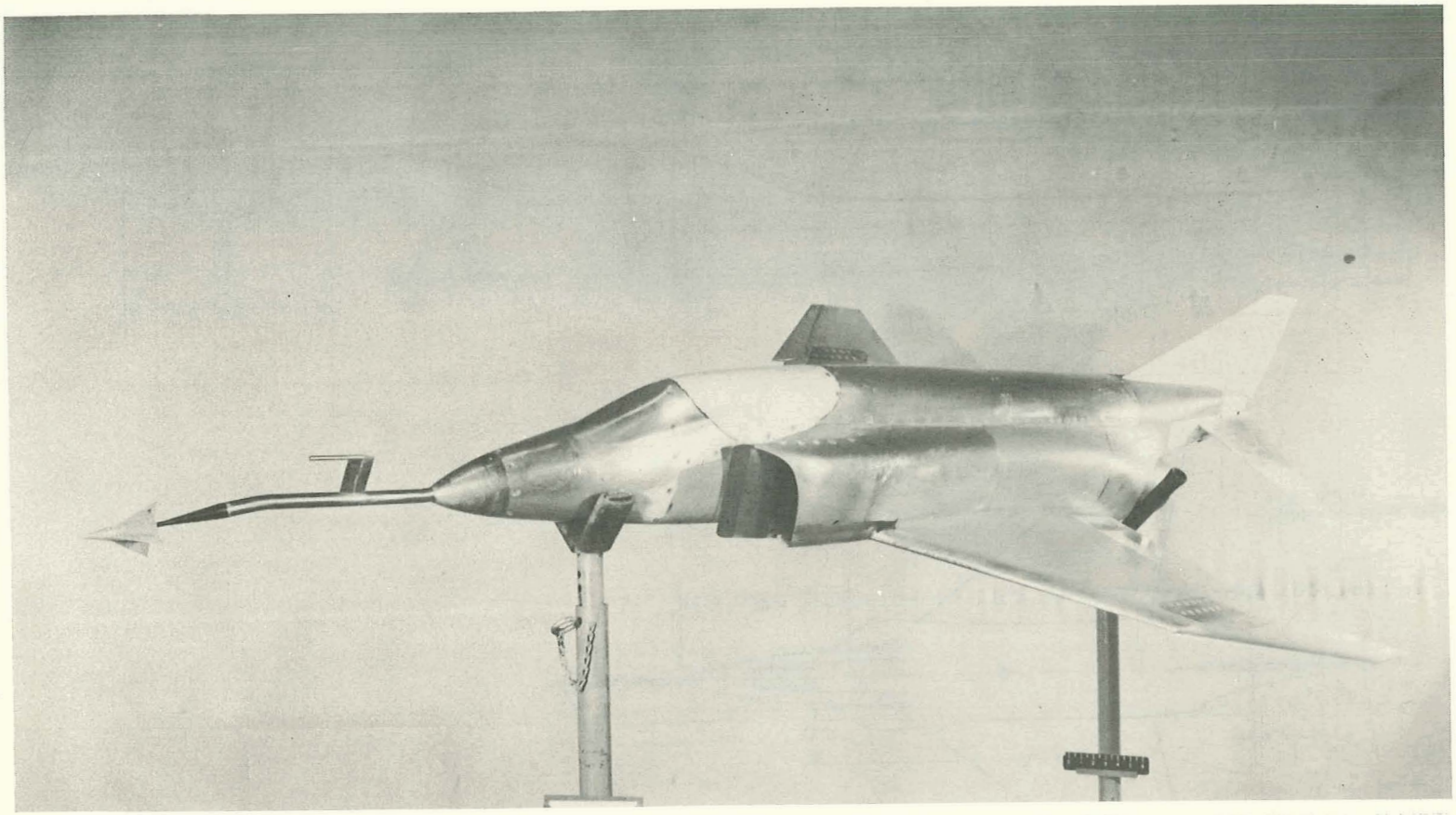

Figure 3.- Photograph of model. L-58-1267

CONFIDENTIAL

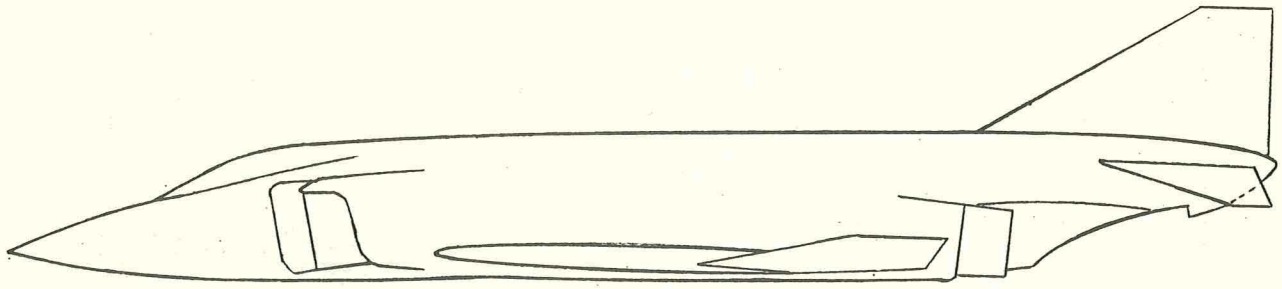

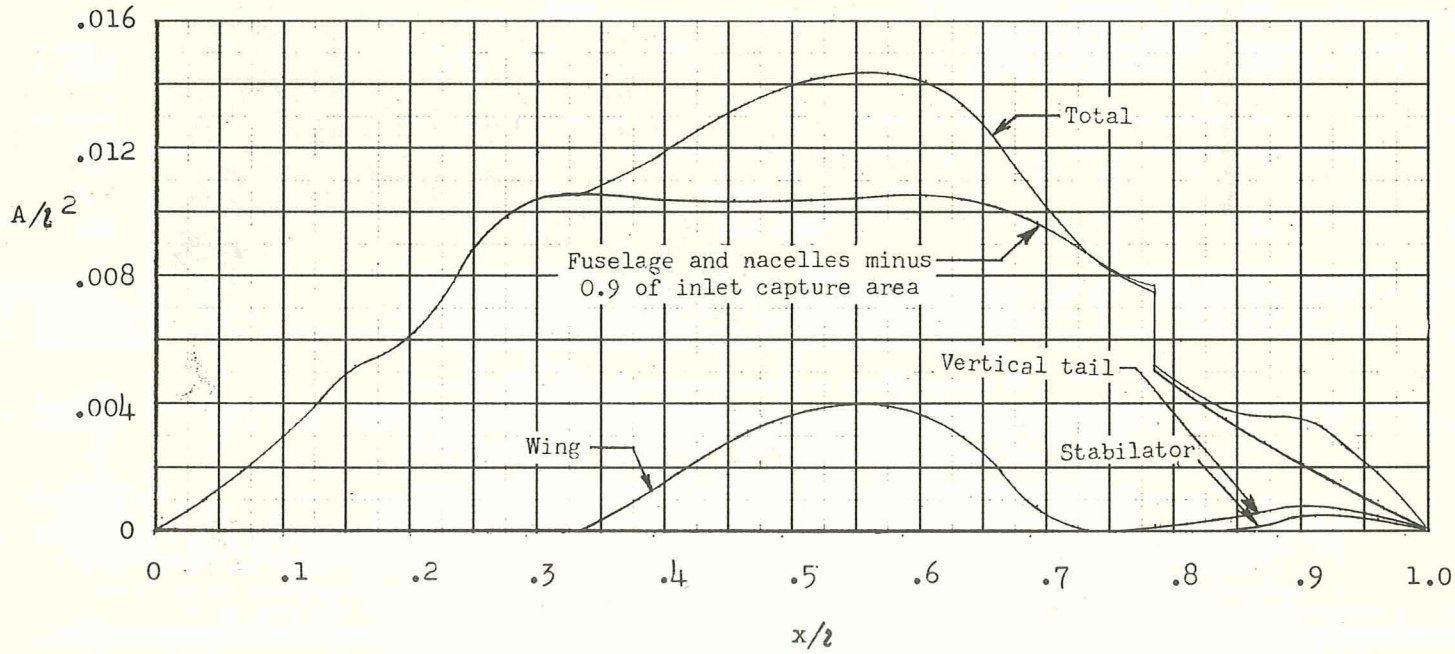

Figure 4.- Normal cross-sectional-area distribution of the model.

CONFIDENTIAL

CONFIDENTIAL

CONFIDENTIAL

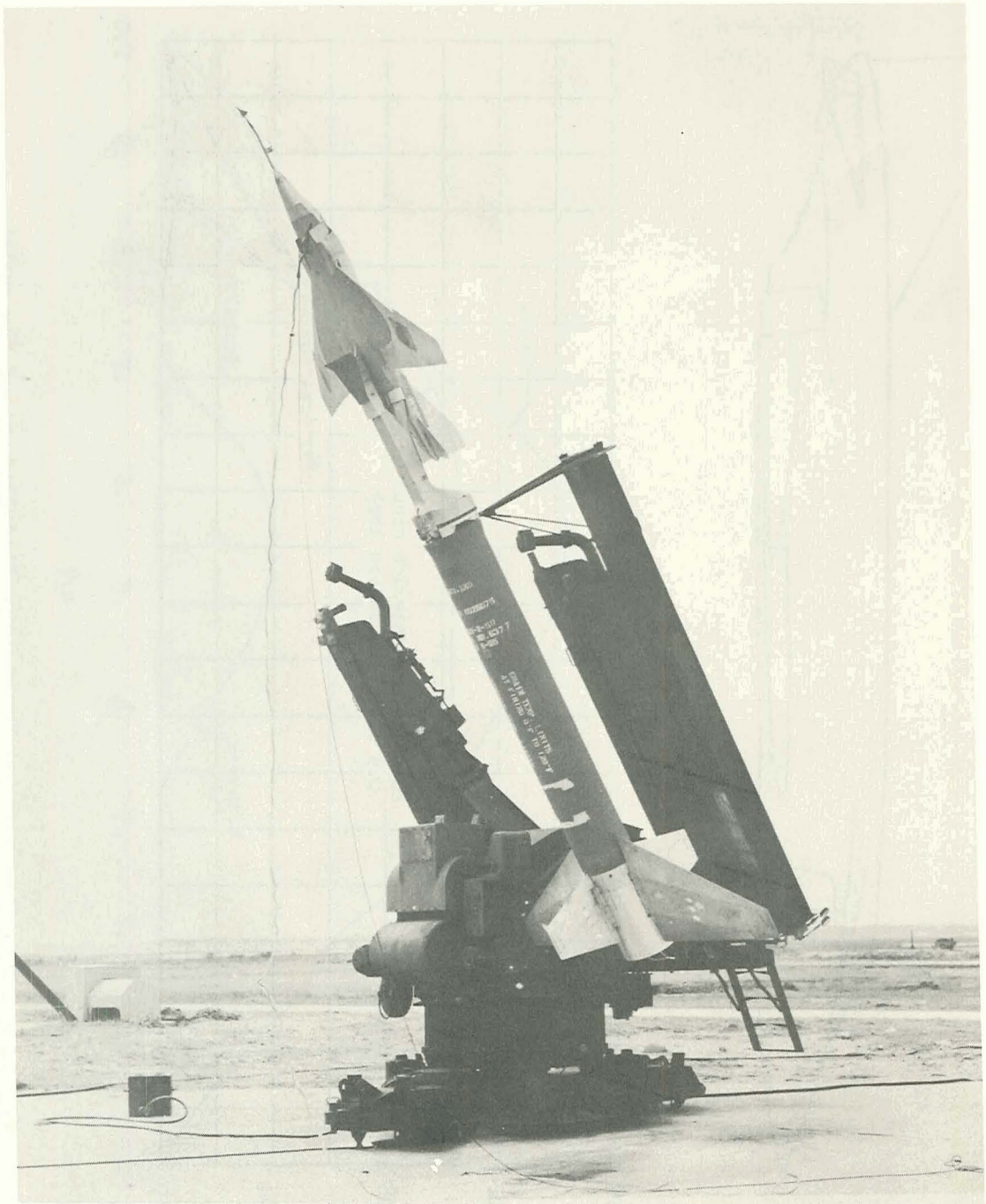

L-58-1811.1

Figure 5.- Photograph of the model-booster combination prior to launching.

CONFIDENTIAL

L-210

CONFIDENTIAL

Figure 6.- Variation of test conditions with Mach number.

CONFIDENTIAL

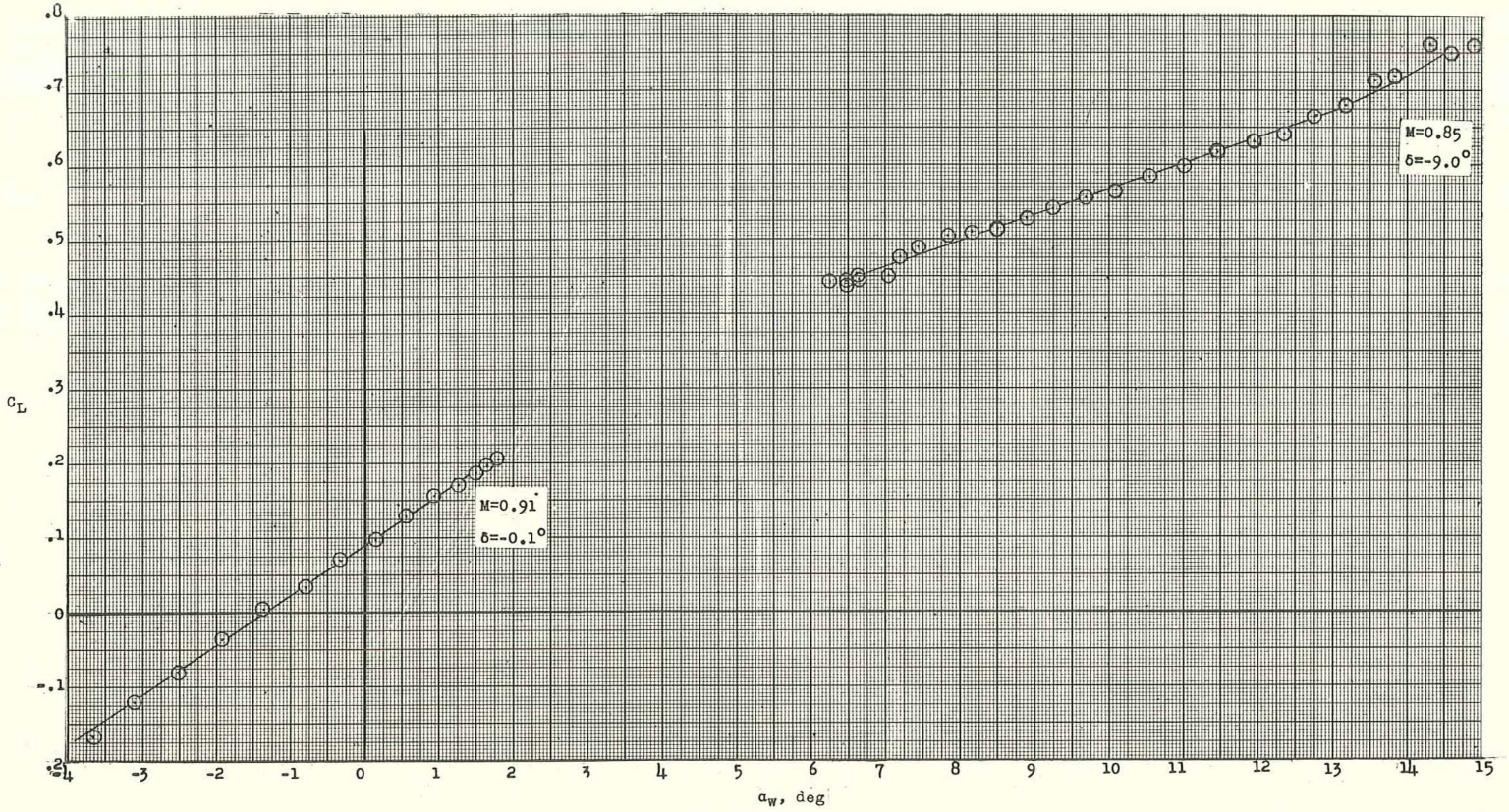

(a) Mach numbers of 0.85 and 0.91

Figure 7.- Variation of lift coefficient with wing angle of attack.

CONFIDENTIAL

CONFIDENTIAL

L-210

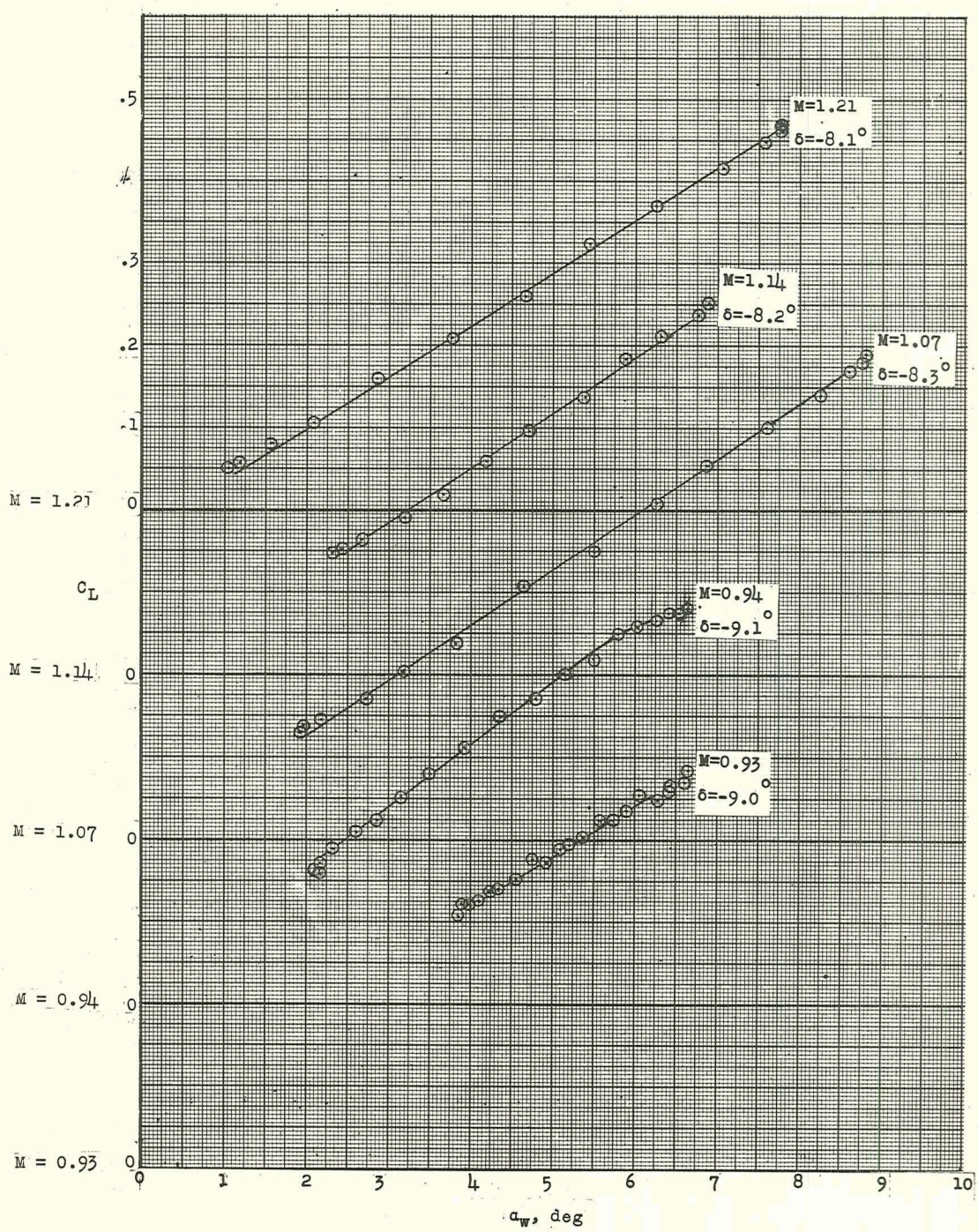

(b) Mach numbers from 0.93 to 1.21.

Figure 7.- Continued.

CONFIDENTIAL

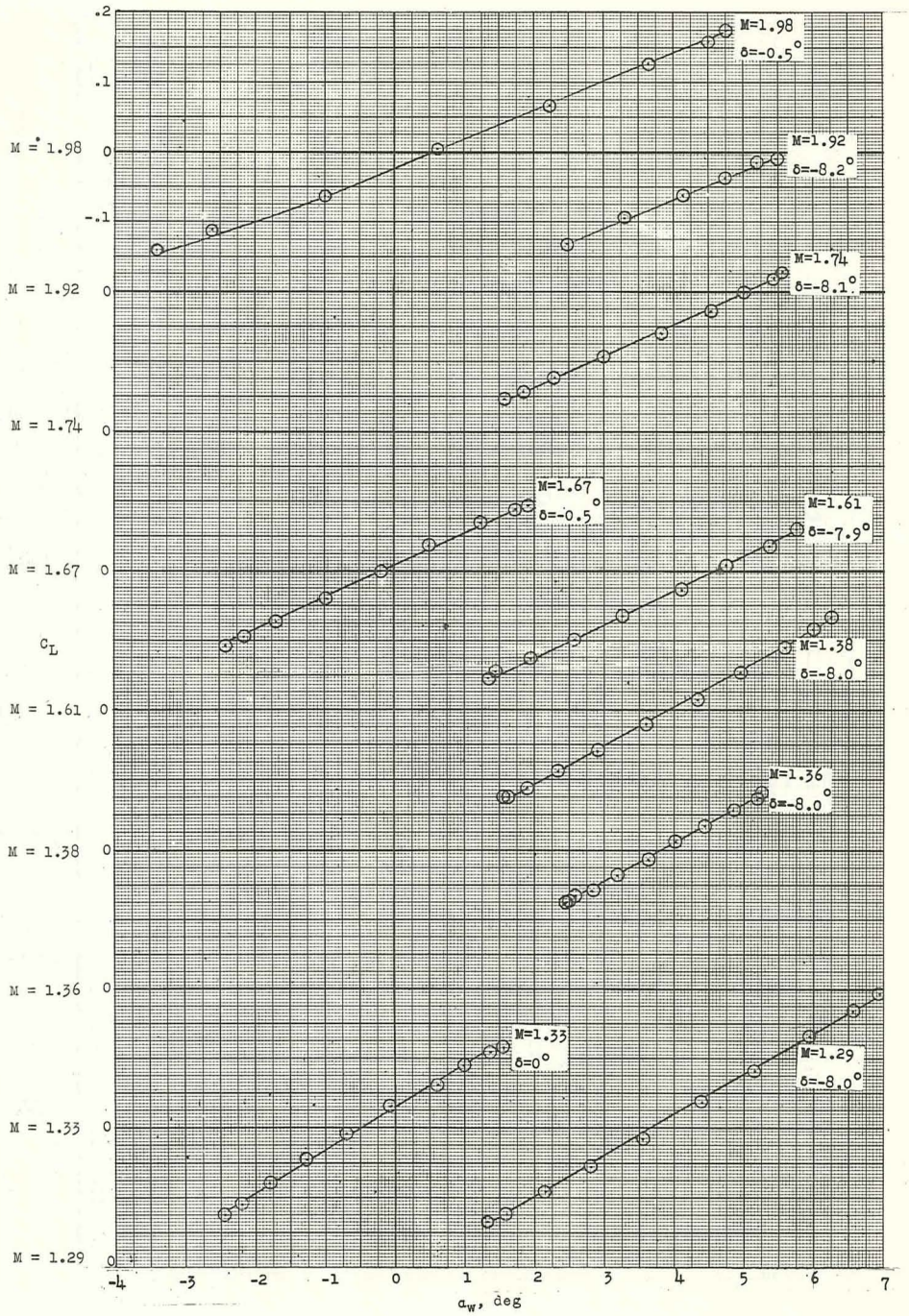

(c) Mach numbers from 1.29 to 1.98.

Figure 7.- Concluded.

CONFIDENTIAL

CONFIDENTIAL

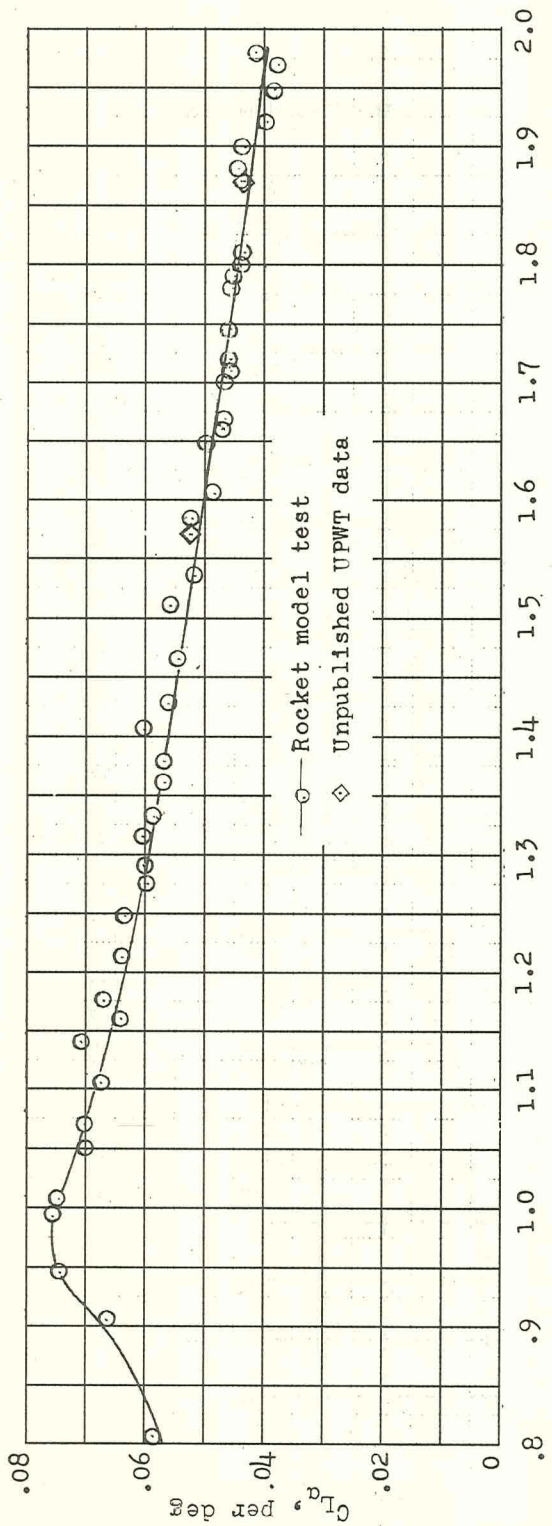

Figure 8.- Lift-curve slope as a function of Mach number.

CONFIDENTIAL

CONFIDENTIAL

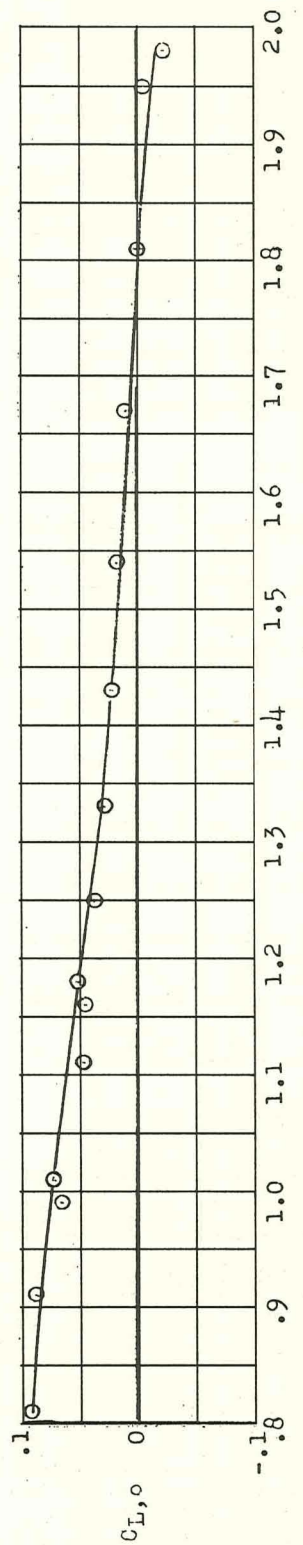

Figure 9.- Basic lift coefficient as a function of Mach number.

CONFIDENTIAL

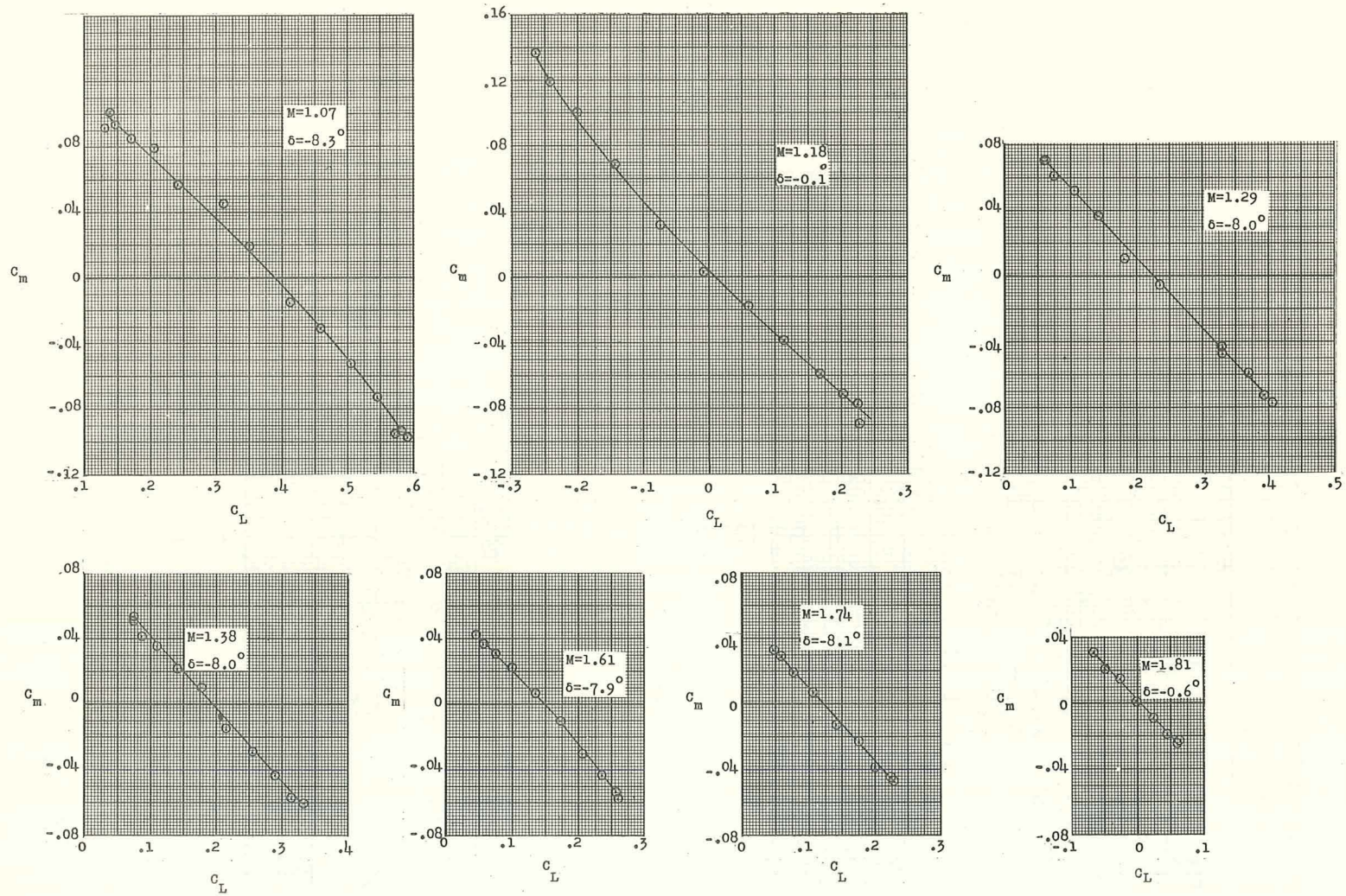

(a) Mach numbers from 1.07 to 1.81.

Figure 10.- Typical variation of pitching-moment coefficient with lift coefficient (center of gravity at $0.199\bar{c}_w$).

CONFIDENTIAL
CONFIDENTIAL

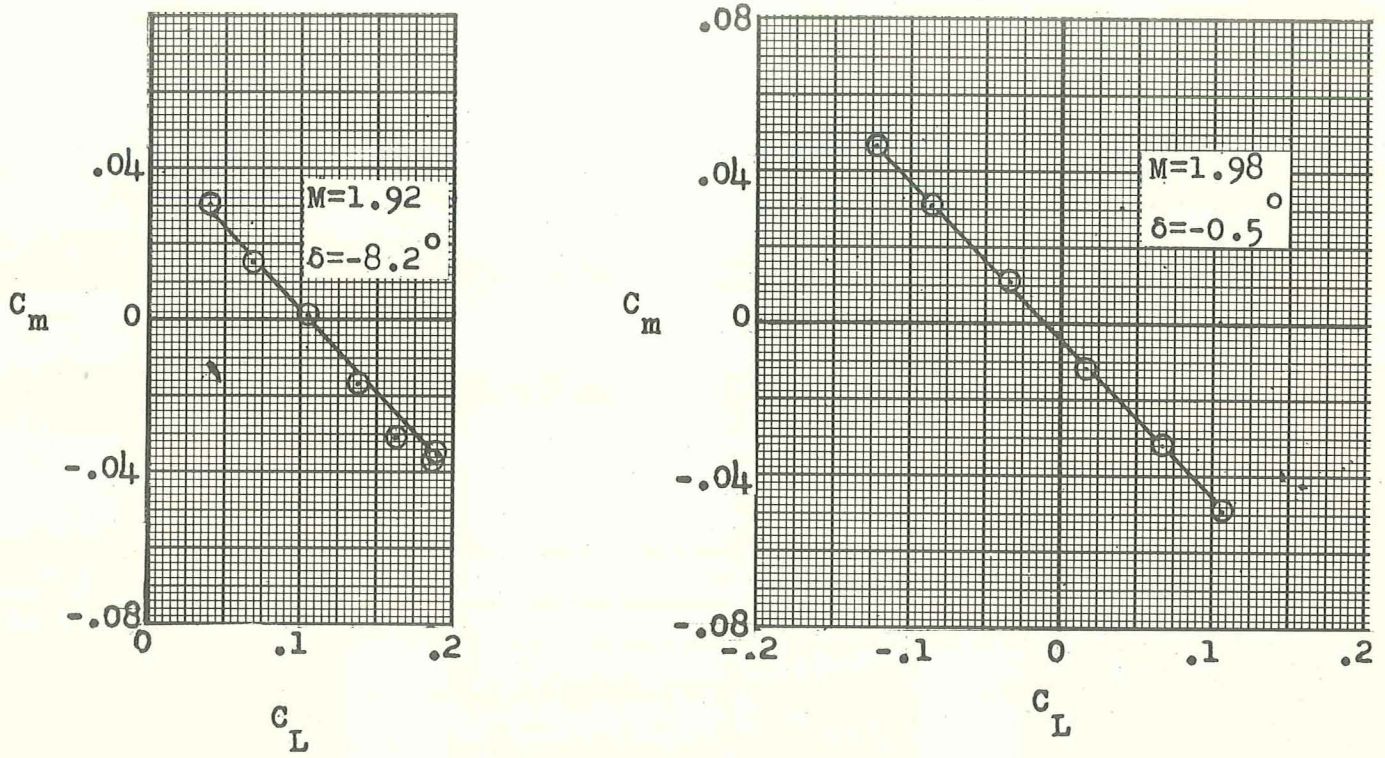

(b) Mach numbers 1.92 and 1.98.

Figure 10.- Concluded.

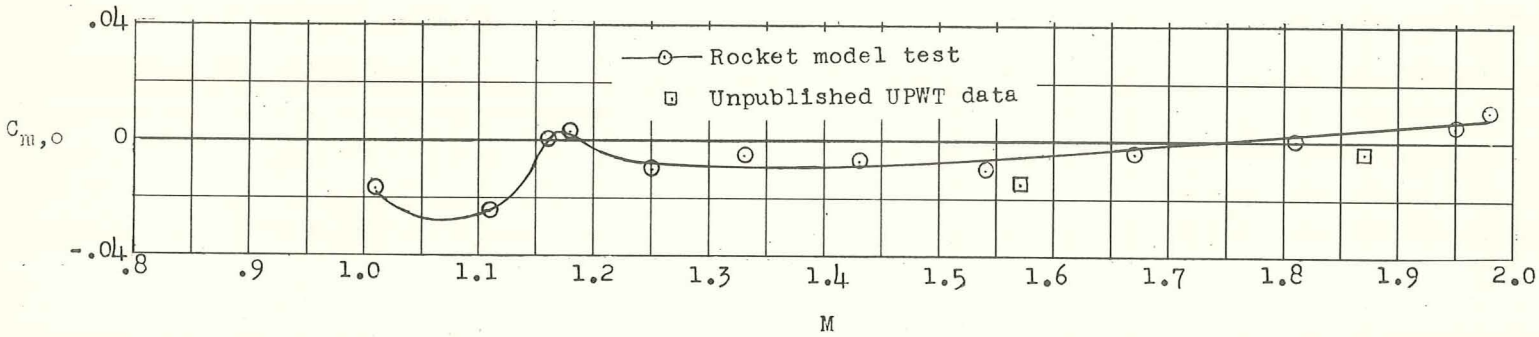

Figure 11.- Variation of basic pitching-moment coefficient with Mach number. Center-of-gravity location at $0.199\bar{c}_w$.

CONFIDENTIAL

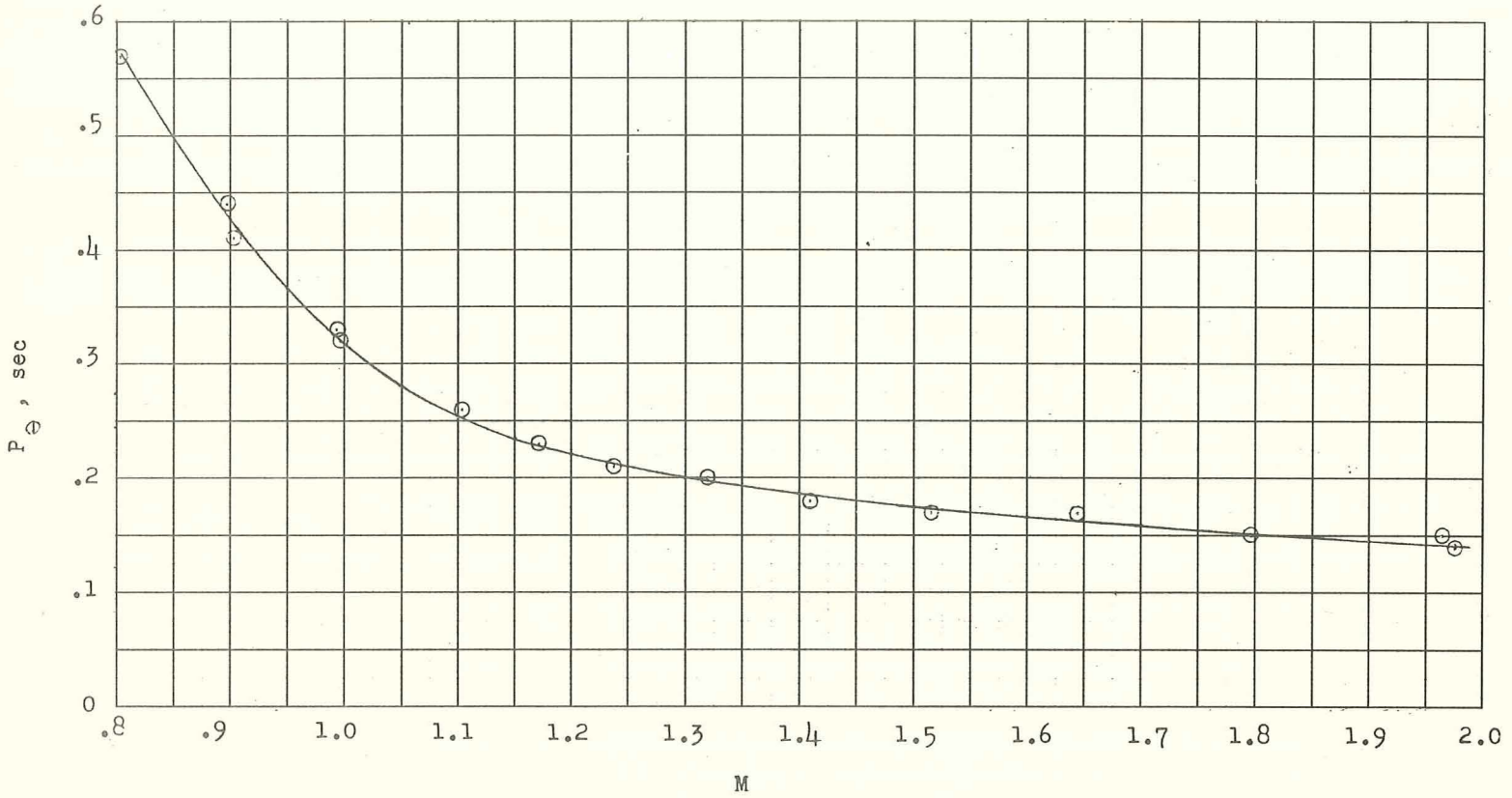

CONFIDENTIAL

Figure 12.- Variation of period in pitch with Mach number.

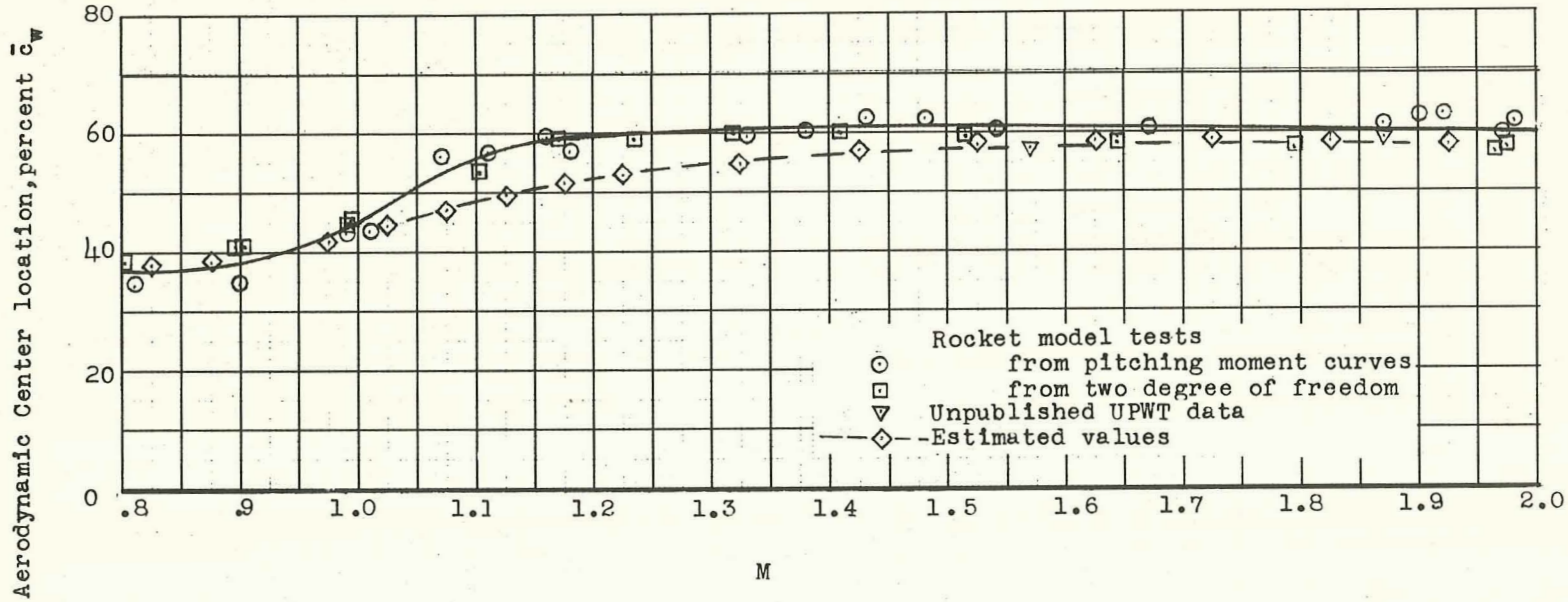

Figure 13.- Variation of aerodynamic-center location with Mach number.

CONFIDENTIAL

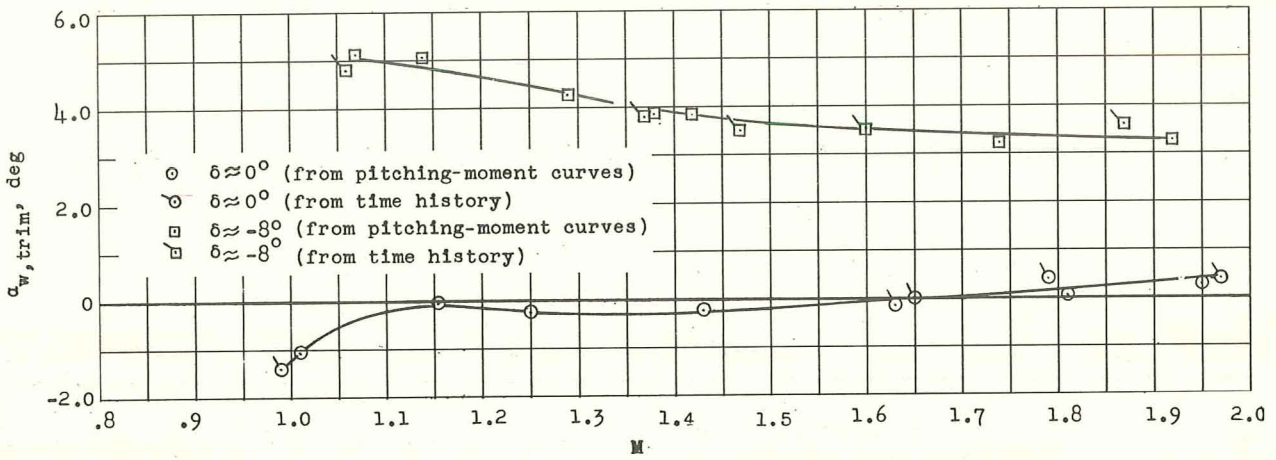

Figure 14.- Variation of trim angle of attack with Mach number. Center-of-gravity location at $0.199\bar{c}_w$.

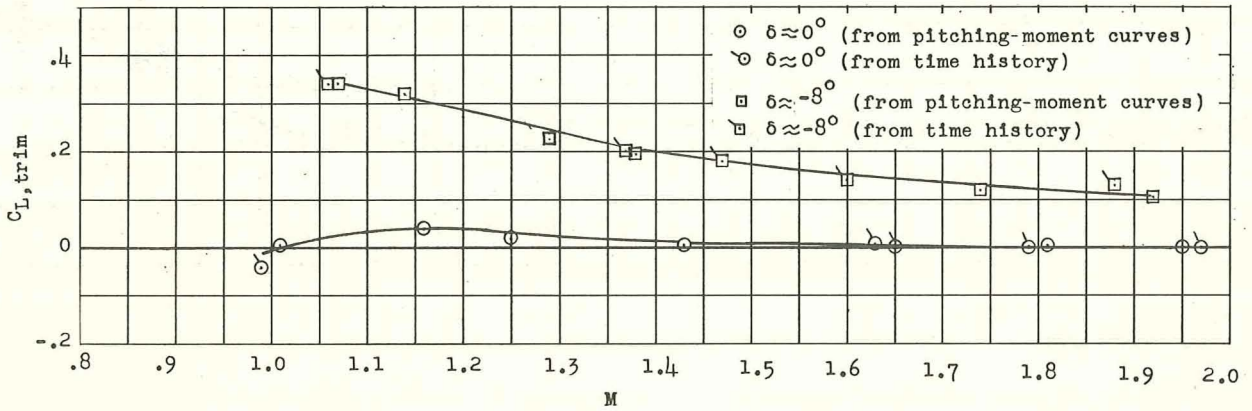

Figure 15.- Variation of trim lift coefficient with Mach number. Center-of-gravity location at $0.199\bar{c}_w$.

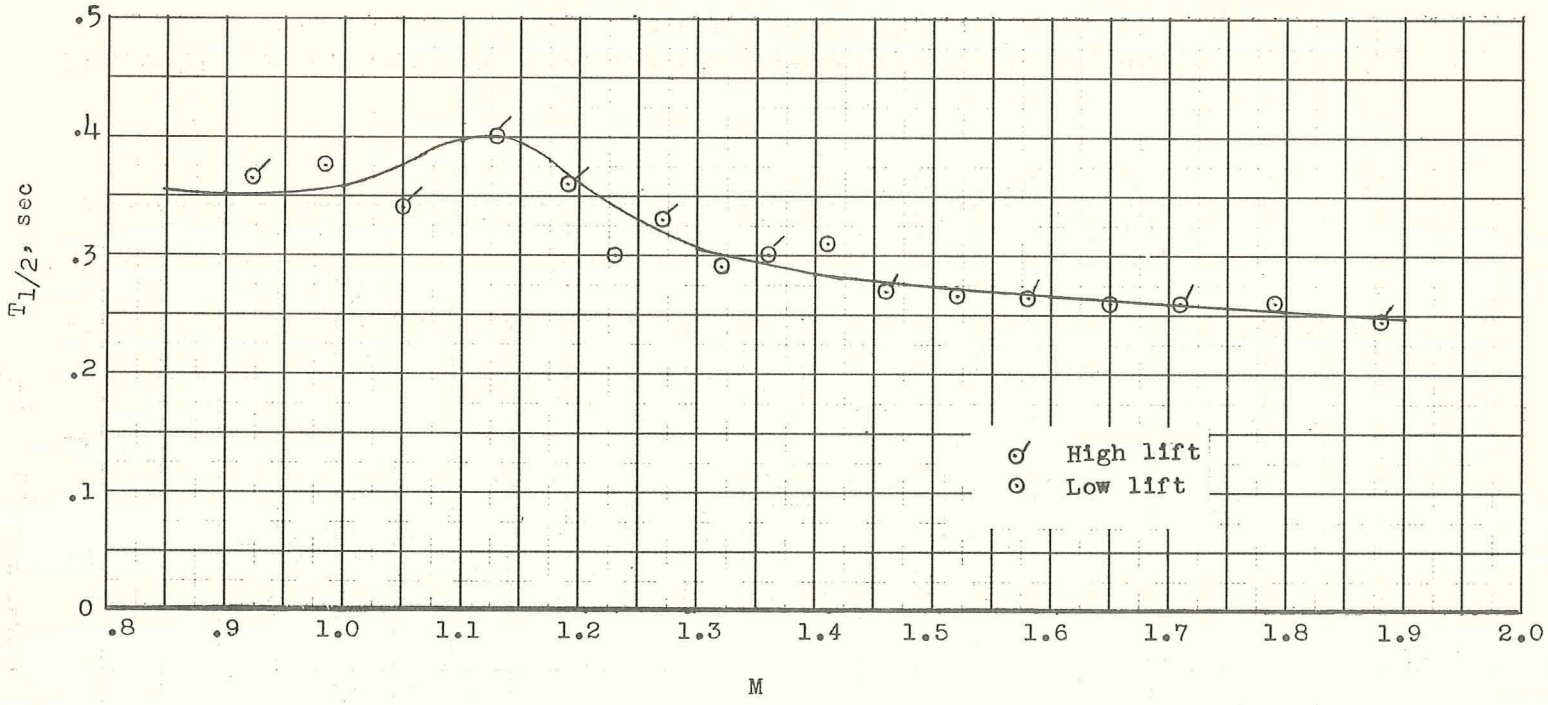

Figure 16.- Time to damp to half amplitude.

CONFIDENTIAL

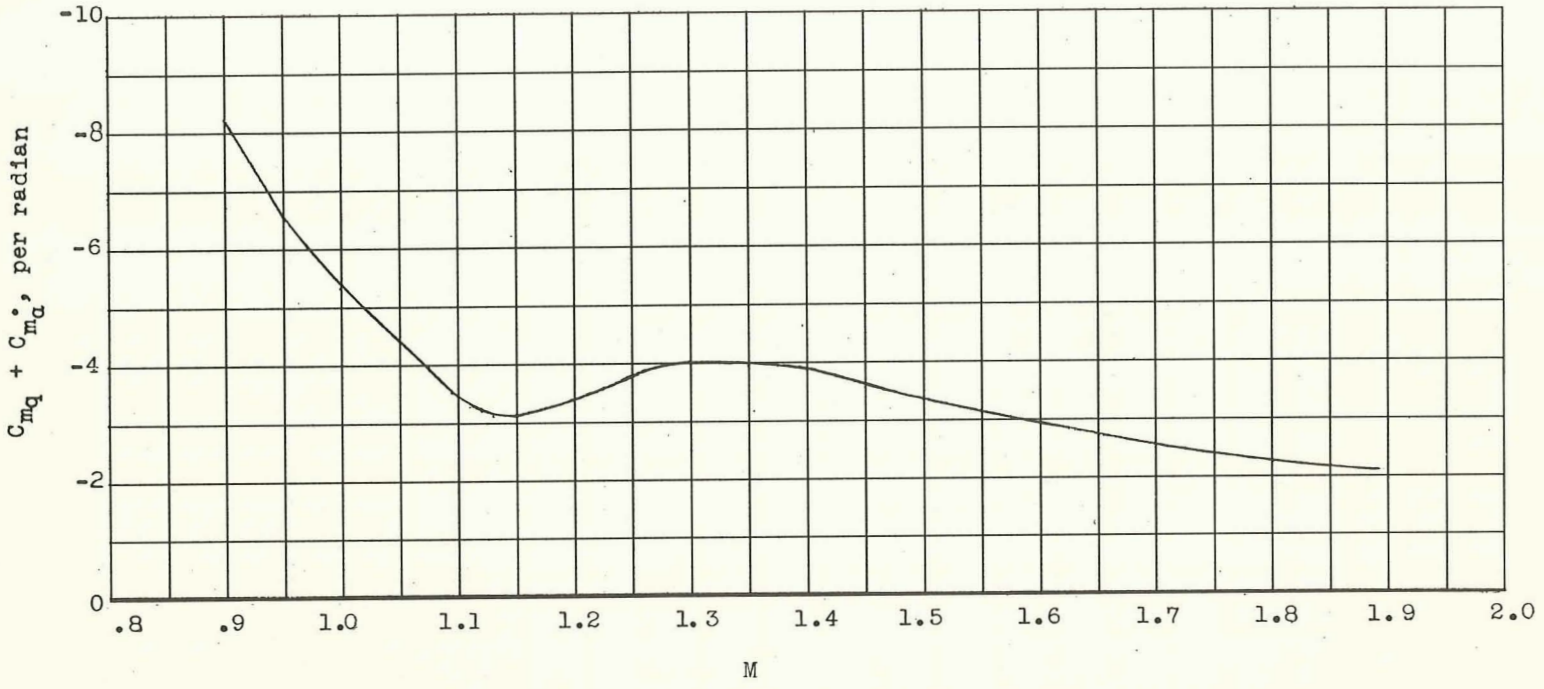

Figure 17.- Variation of damping-in-pitch derivative with Mach number. Center-of-gravity location at $0.199\bar{c}_w$.

CONFIDENTIAL

CONFIDENTIAL

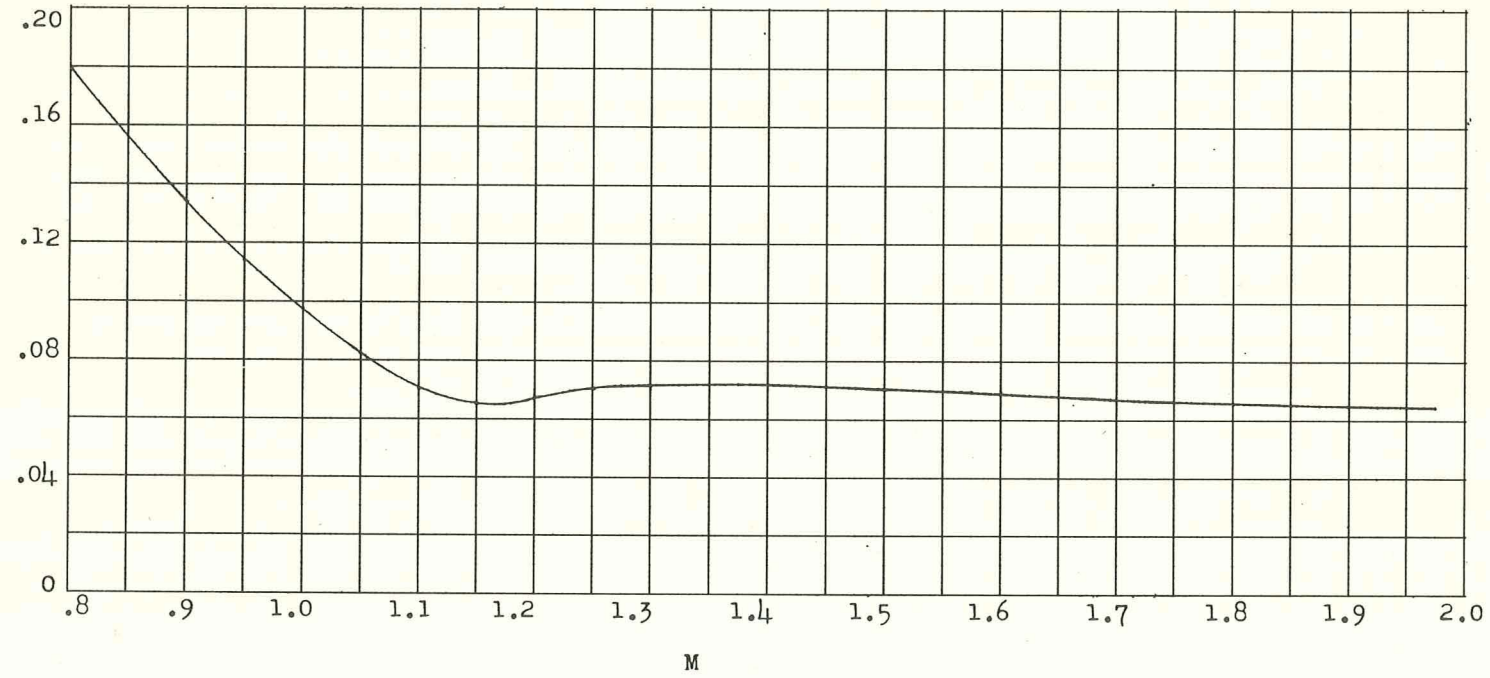

Figure 18.- Variation of critical-damping ratio with Mach number.

CONFIDENTIAL

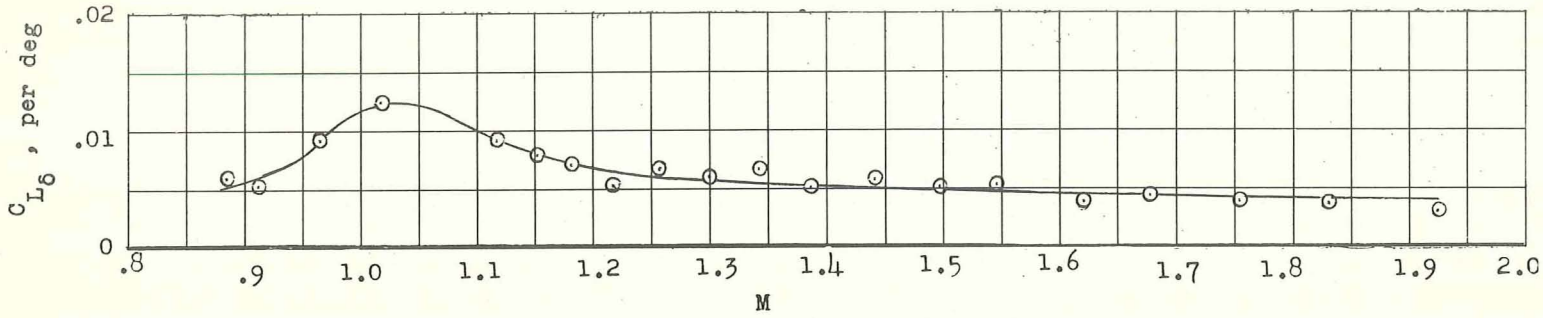

Figure 19.- Variation of stabilator lift effectiveness with Mach number.

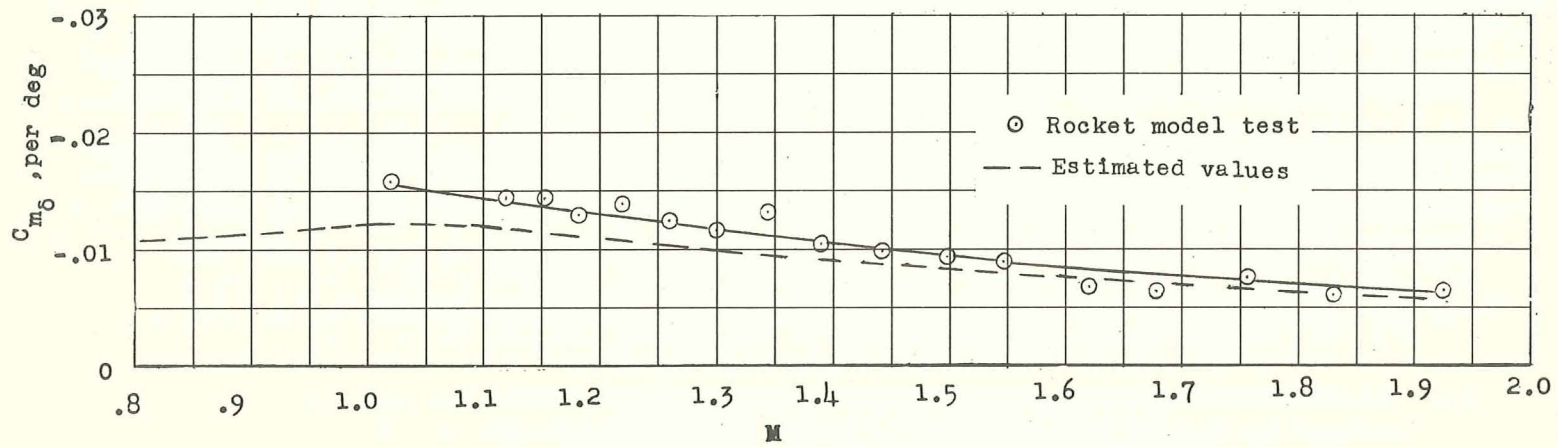

Figure 20.- Variation of stabilator pitching effectiveness with Mach number. Center-of-gravity location at $0.199\bar{c}_w$.

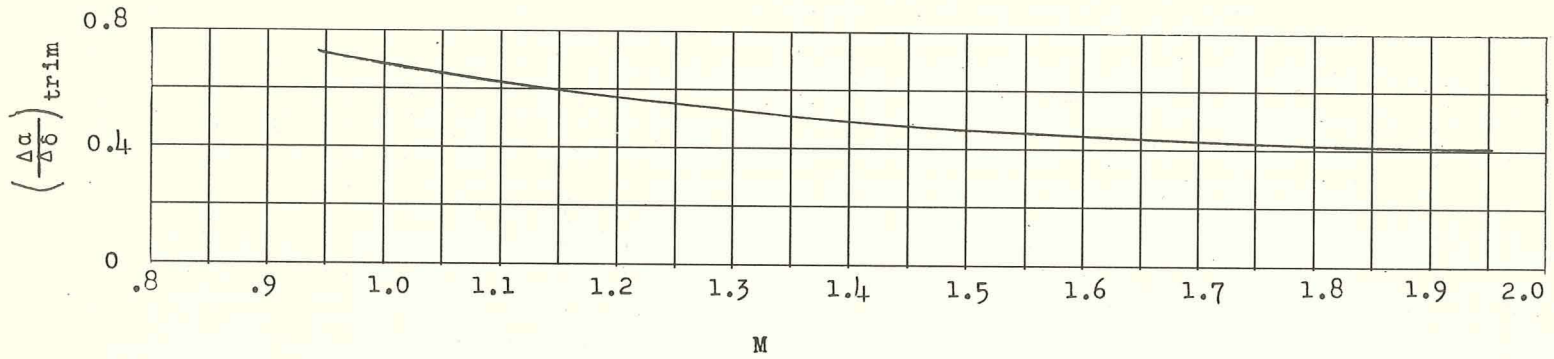

Figure 21.- Change in trim angle of attack per degree of stabilator deflection.

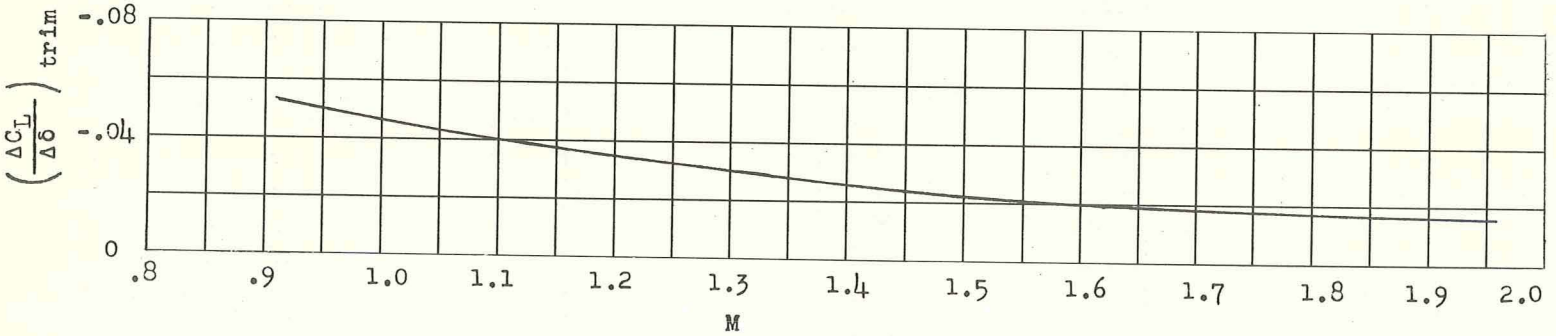

Figure 22.- Change in trim lift coefficient per degree of stabilator deflection.

CONFIDENTIAL

CONFIDENTIAL

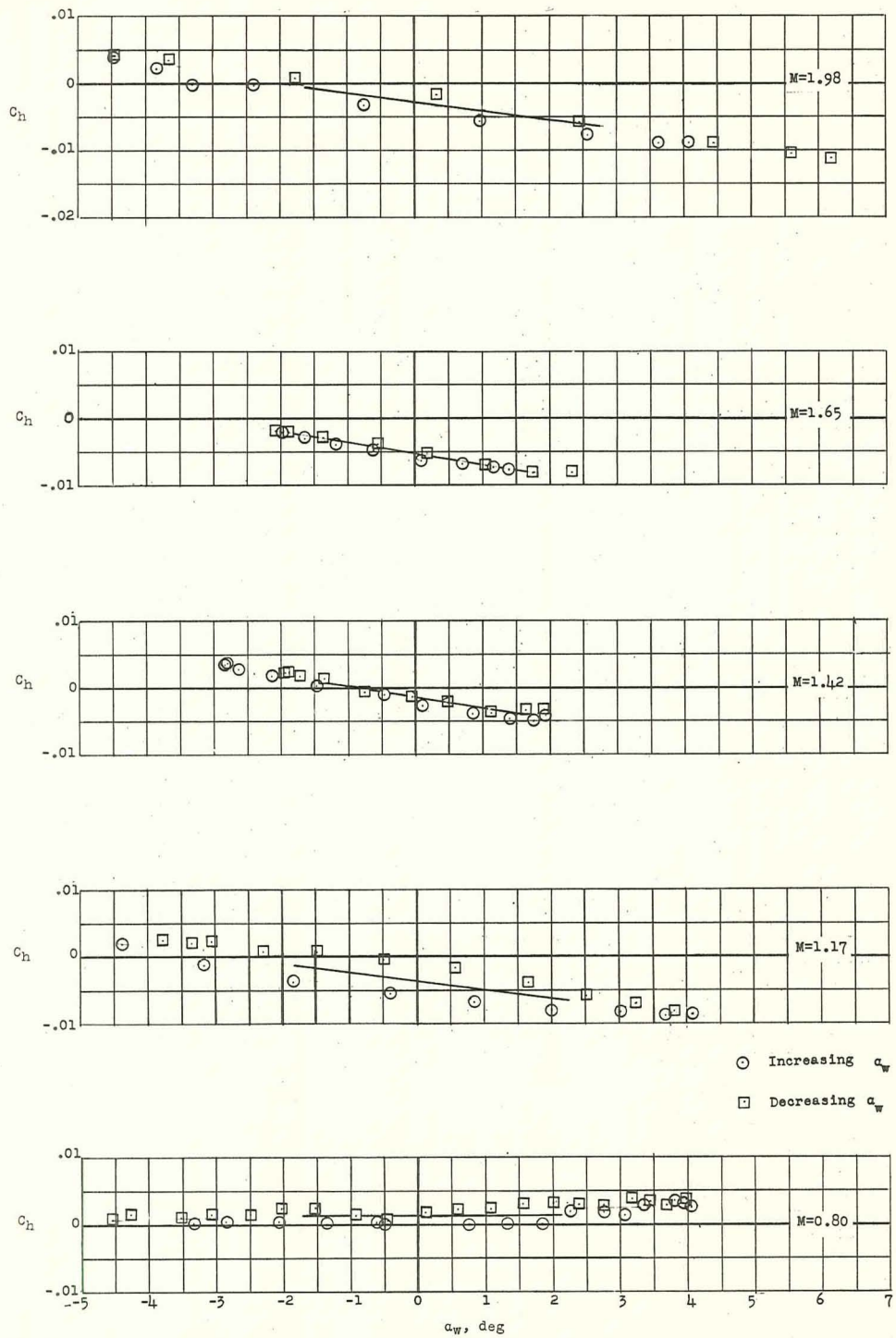

Figure 23.- Typical variation of hinge-moment coefficient with angle of attack at $\delta \approx 0^\circ$.

CONFIDENTIAL

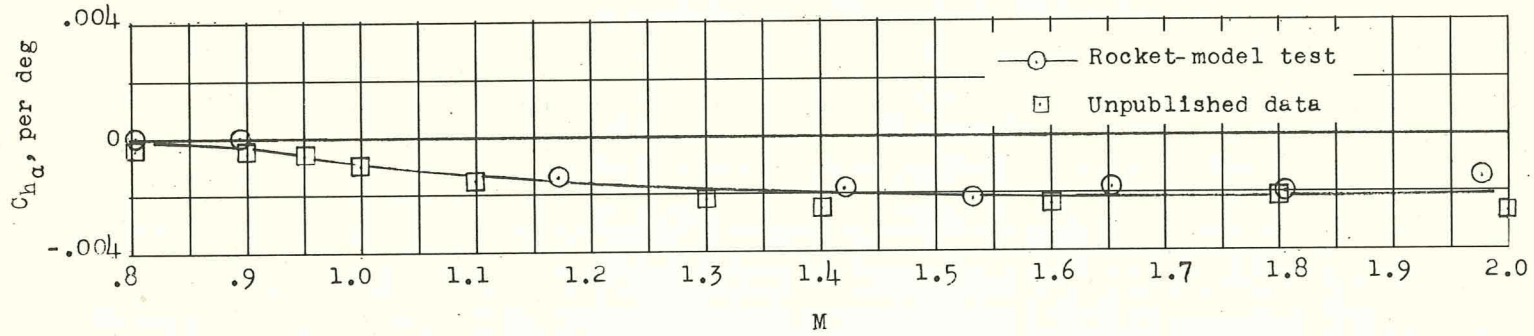

Figure 24.- Effect of Mach number on C_{h_α}.

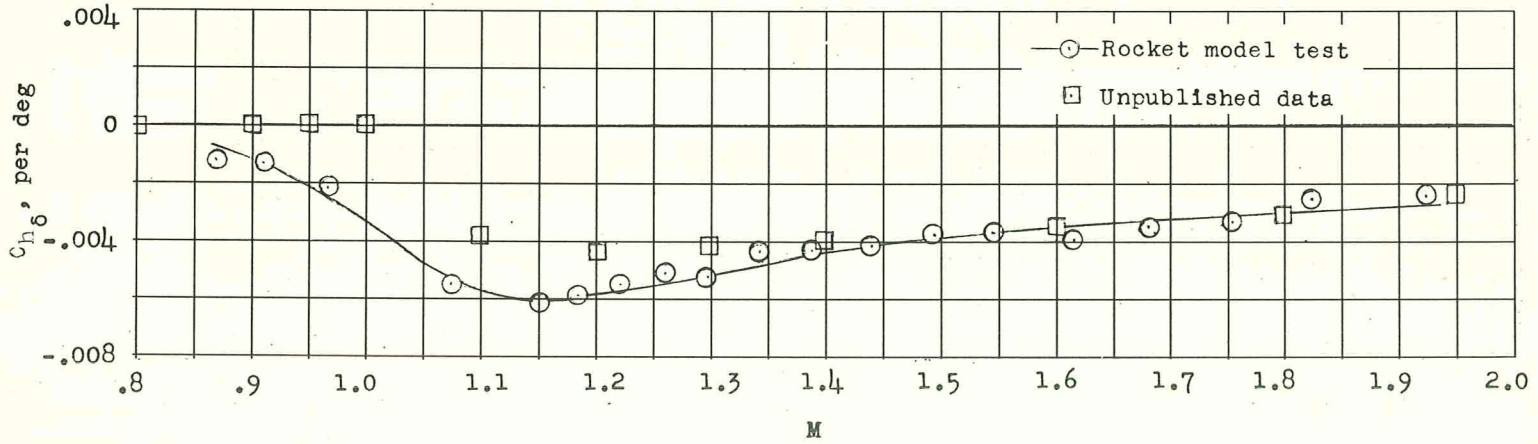

Figure 25.- Effect of Mach number on C_{h_δ}.

CONFIDENTIAL

CONFIDENTIAL

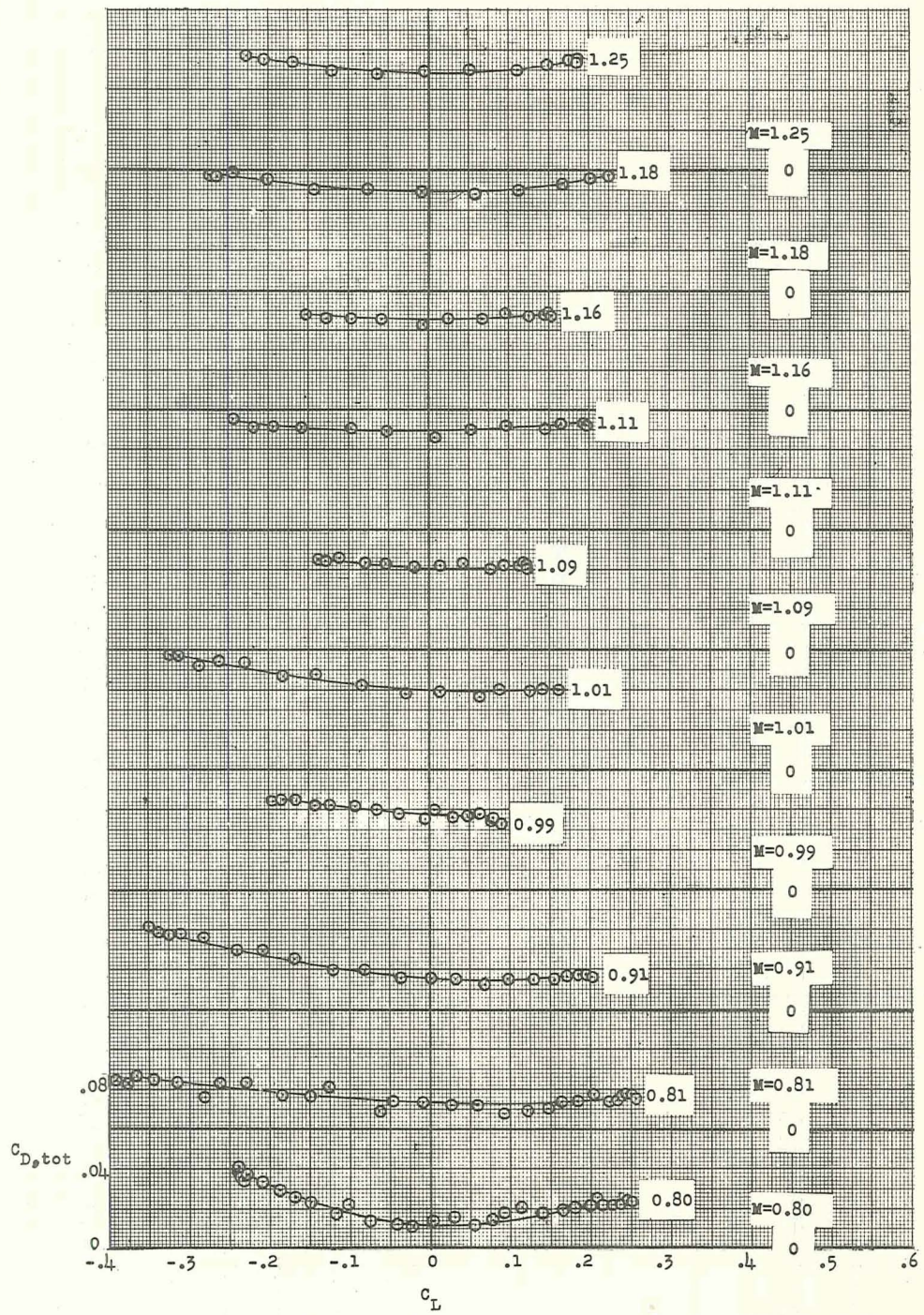

(a) Mach numbers from 0.80 to 1.25. $\delta \approx 0^{\circ}$.

Figure 26.- Variation of total drag coefficient with lift coefficient.

CONFIDENTIAL

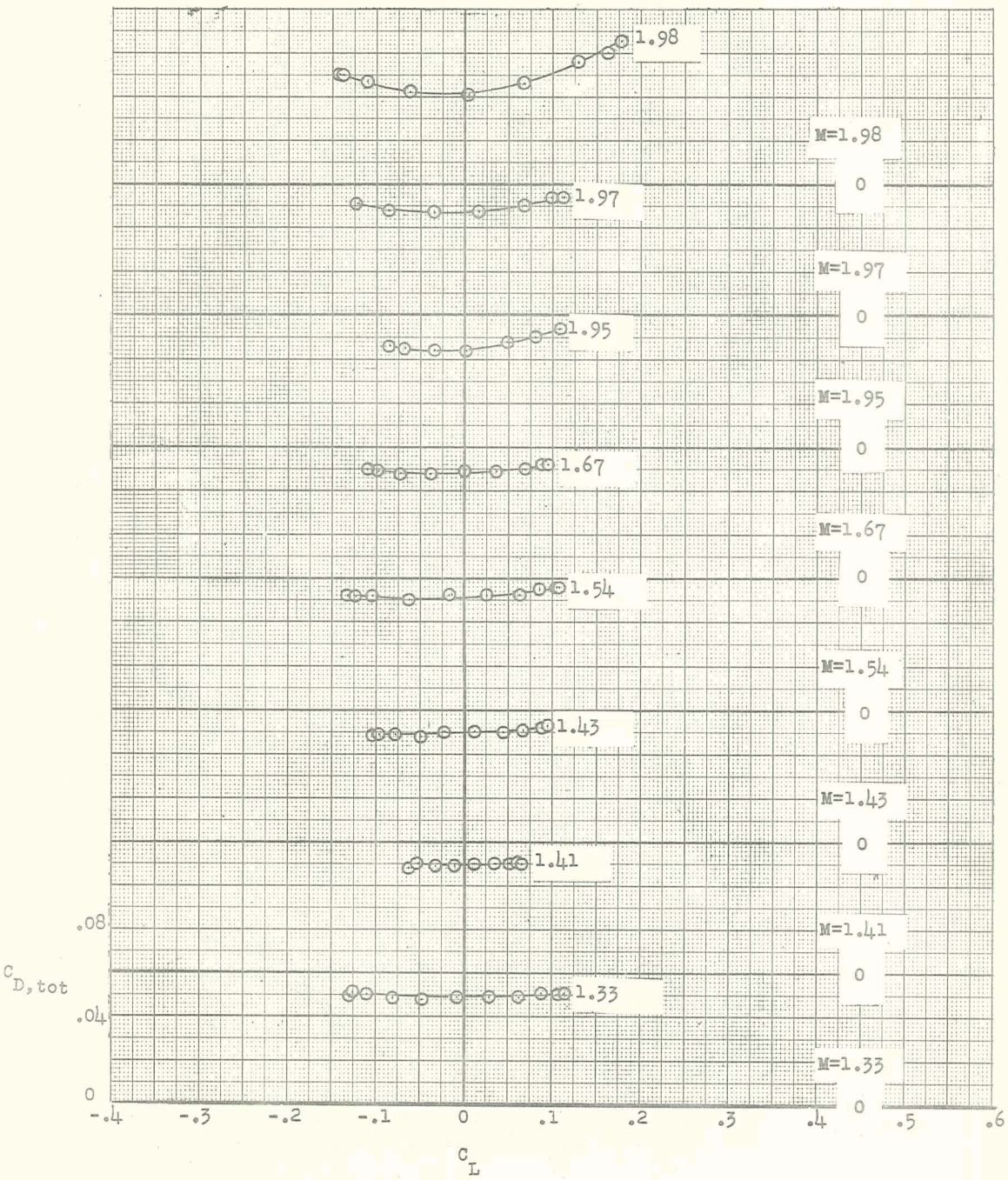

(b) Mach numbers from 1.33 to 1.98. $\delta \approx 0^{\circ}$.

Figure 26.- Continued.

CONFIDENTIAL

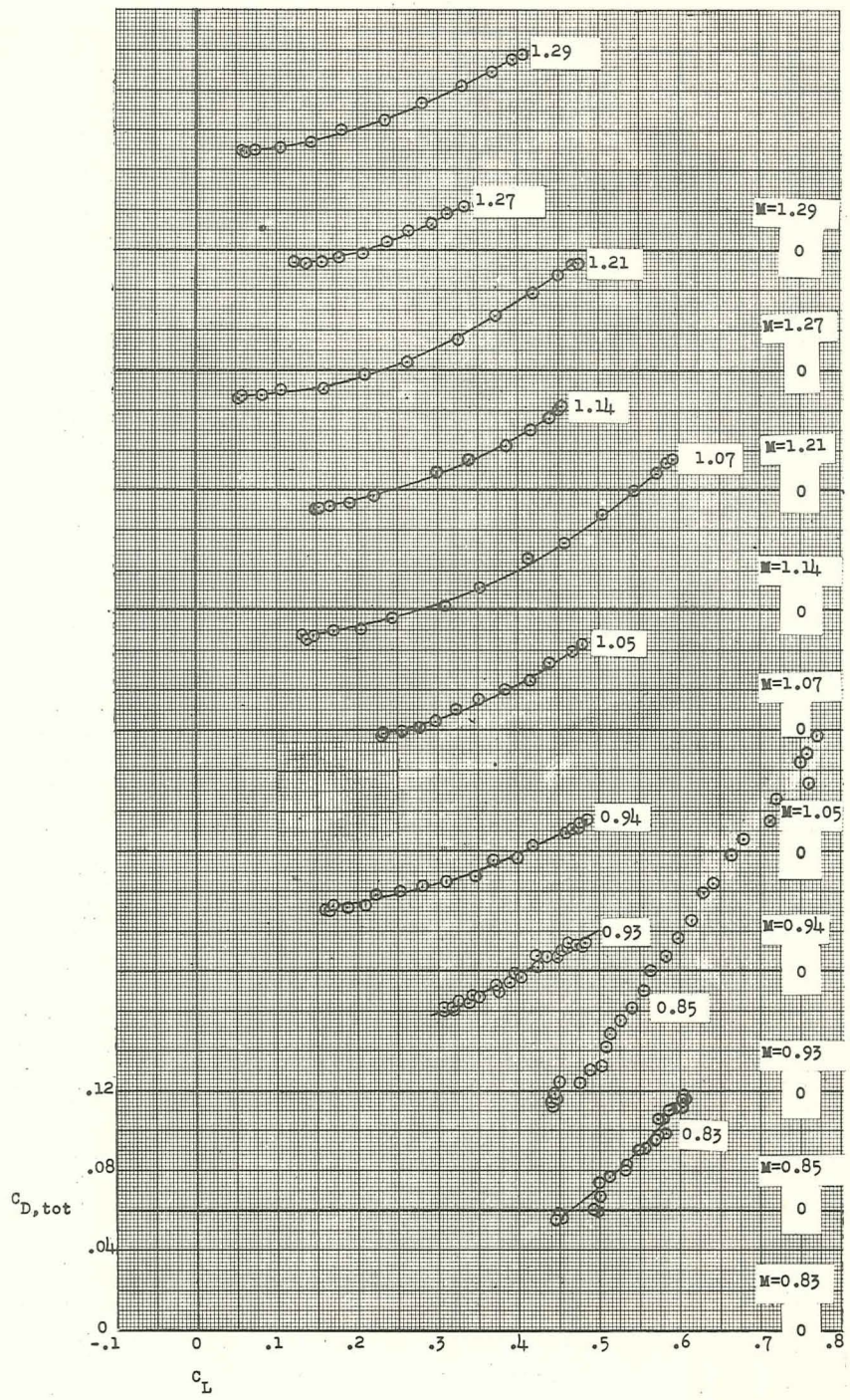

(c) Mach numbers from 0.83 to 1.29. $\delta \approx -8^{\circ}$.

Figure 26.- Continued.

CONFIDENTIAL

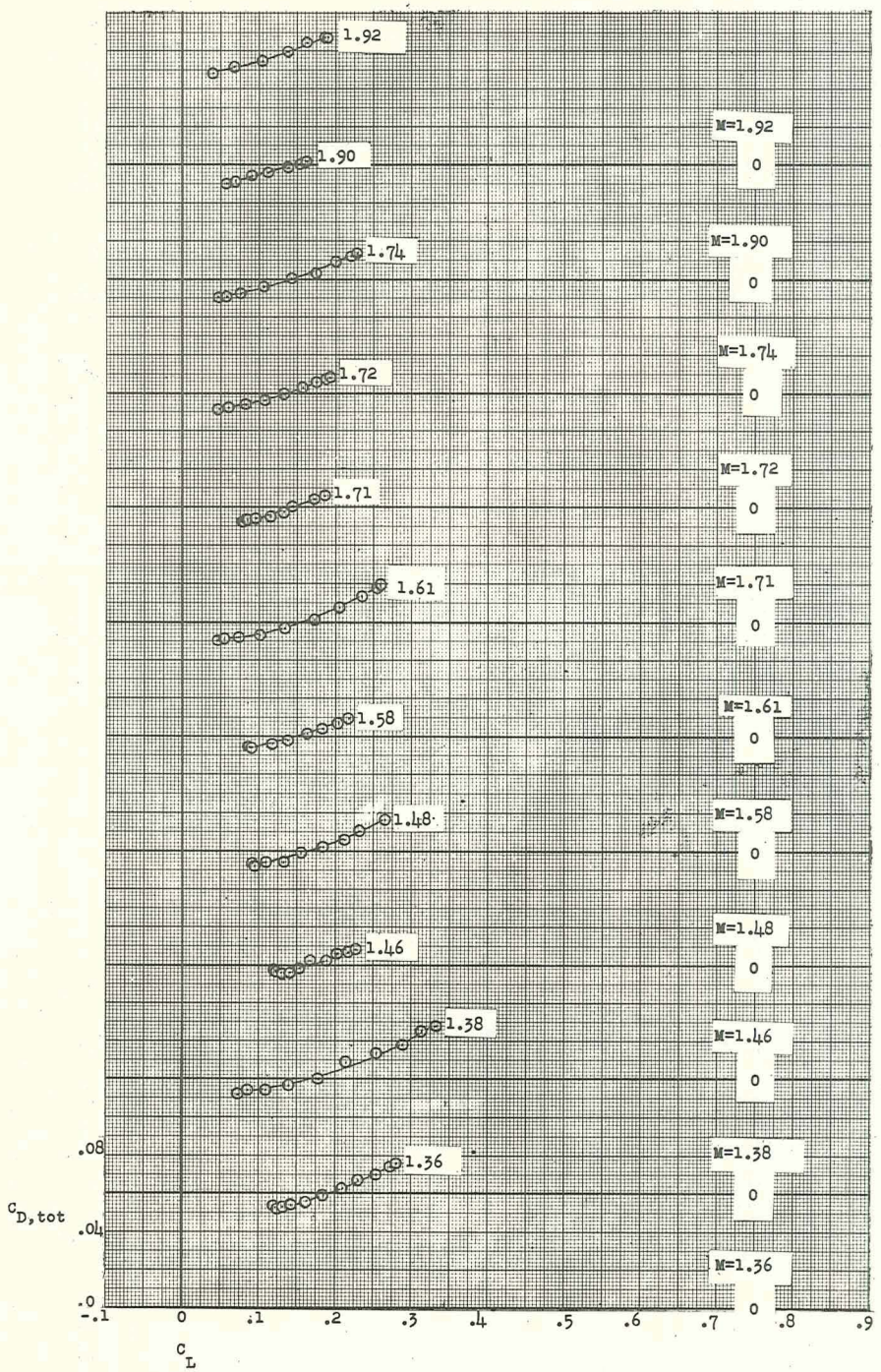

(d) Mach numbers from 1.36 to 1.92. $\delta \approx -8^{\circ}$.

Figure 26.- Concluded.

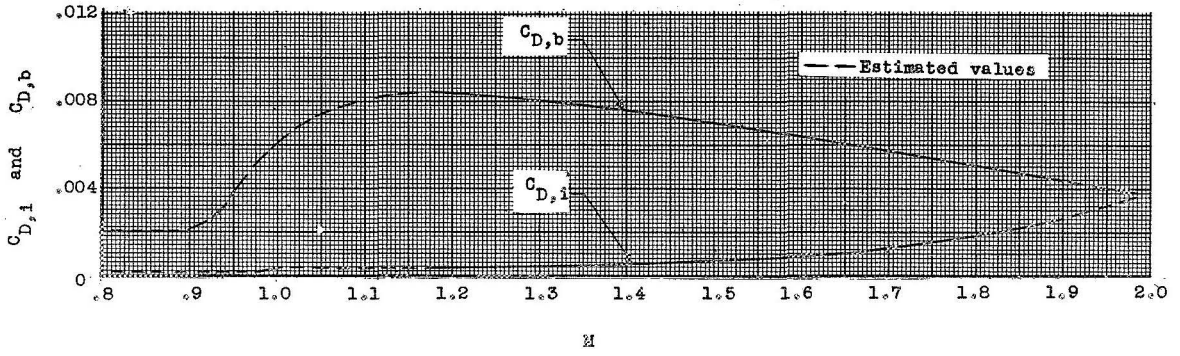

Figure 27.- Internal and base drag coefficients obtained from a rocket model test of a configuration with identical internal and base geometry.

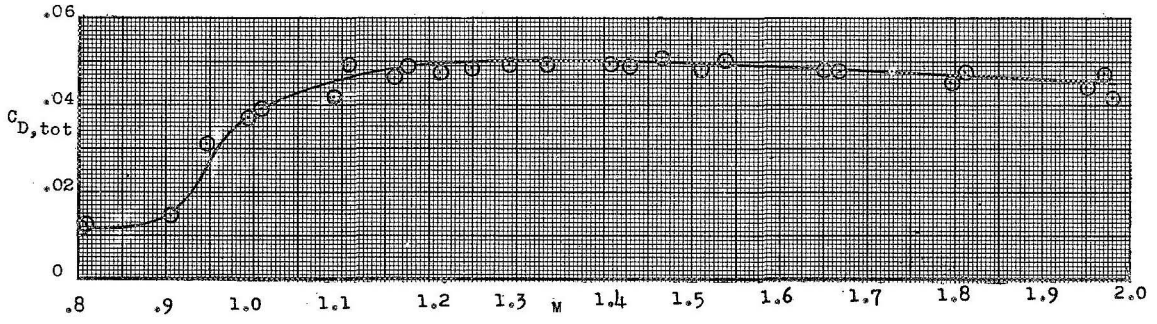

Figure 28.- Variation of minimum total-drag coefficient (including internal and base drag) with Mach number.

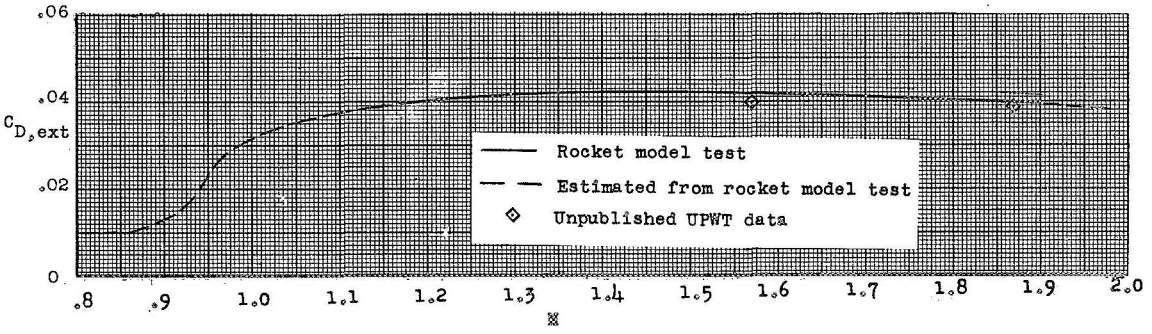

Figure 29.- Variation of minimum external-drag coefficient with Mach number.

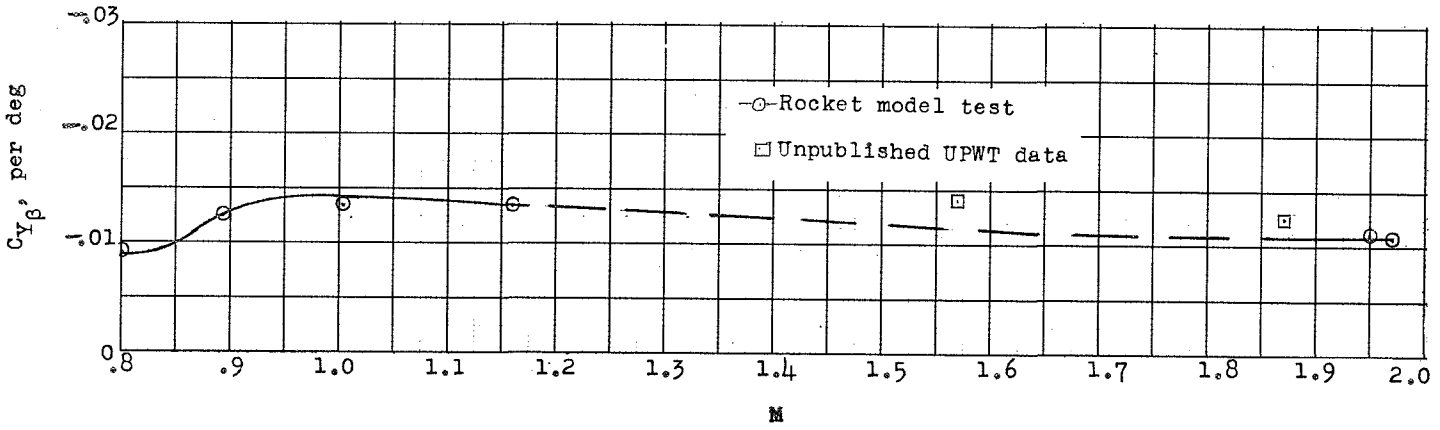

Figure 30.- Variation of side-force derivative with Mach number.

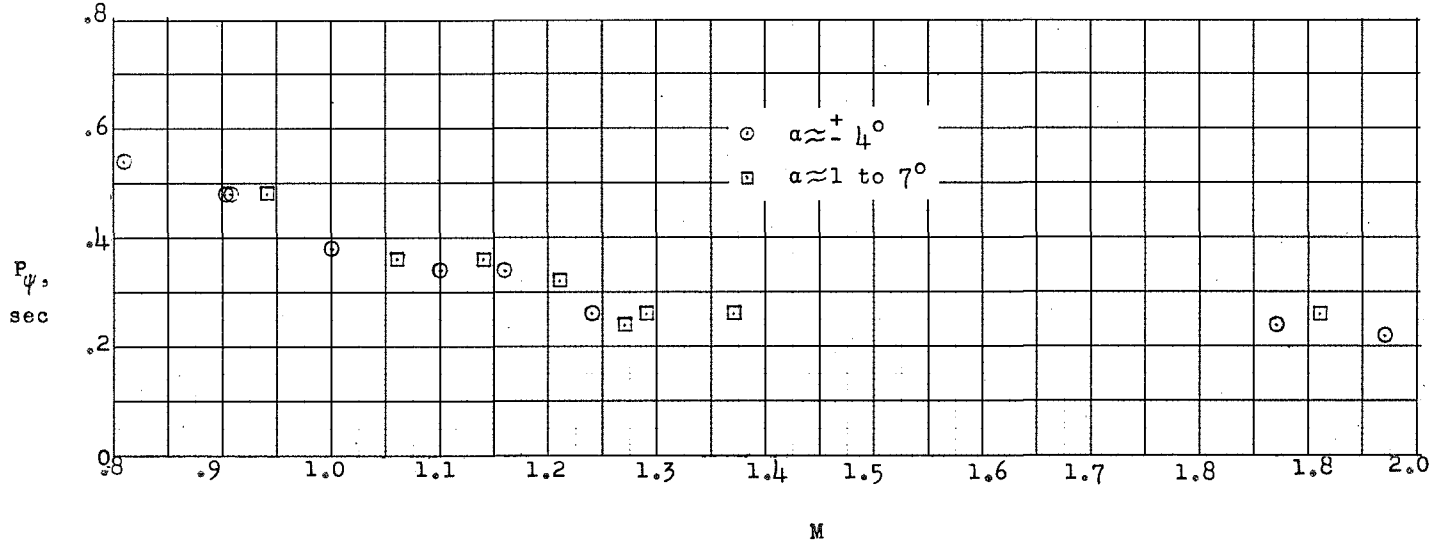

Figure 31.- Variation of period in yaw with Mach number.

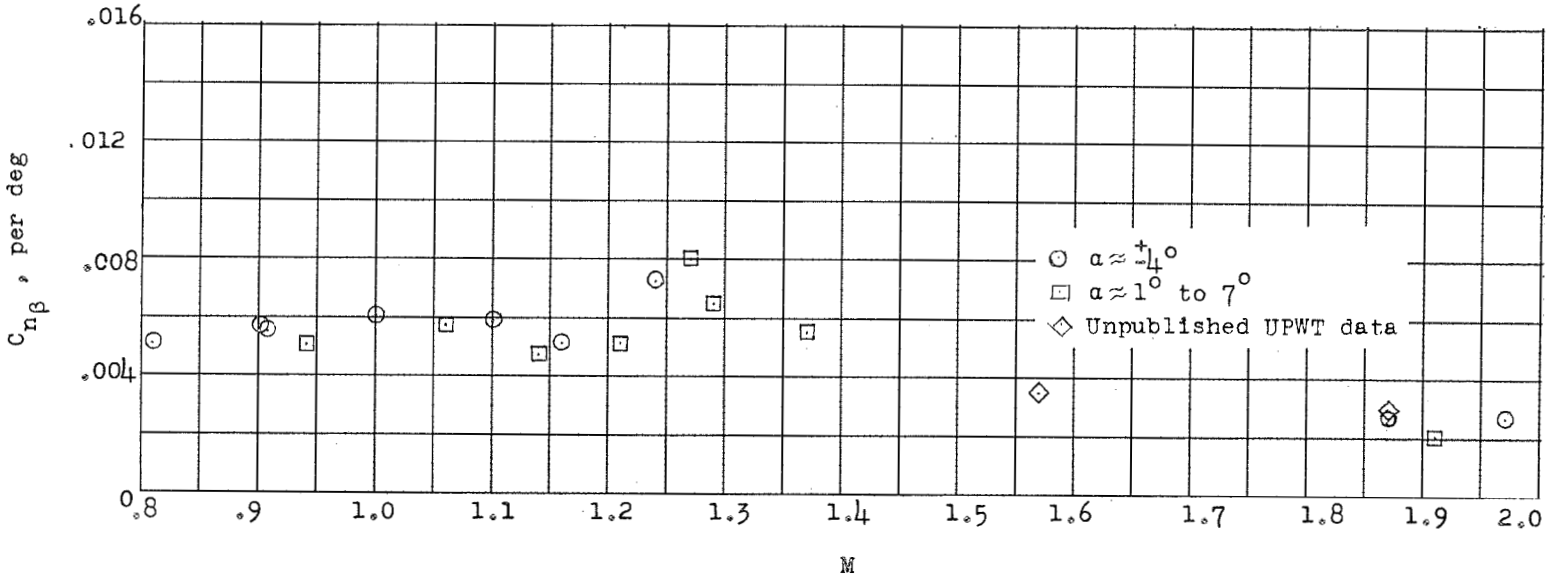

Figure 32.- Variation of static-directional-stability parameter with Mach number.

CONFIDENTIAL

CONFIDENTIAL